2007

Neurodegeneration and Neuroinflammation in a Mouse Model of Sarin Exposure

Molly Elizabeth Davidson
Wright State University

NEURODEGENERATION AND NEUROINFLAMMATION IN A MOUSE MODEL OF SARIN EXPOSURE

A thesis submitted in partial fulfillment
of the requirements for the degree of
Master of Science

By

MOLLY ELIZABETH DAVIDSON
B.S., University of Dayton, 2003

2007
Wright State University

WRIGHT STATE UNIVERSITY

SCHOOL OF GRADUATE STUDIES

September 4, 2007

I HEREBY RECOMMEND THAT THE THESIS PREPARED UNDER MY SUPERVISION BY Molly Elizabeth Davidson ENTITLED Neurodegeneration and Neuroinflammation in a Mouse Model of Sarin Exposure BE ACCEPTED IN PARTIAL FULFILLMENT OF THE REQUIREMENTS FOR THE DEGREE OF Master of Science.

_____

David R. Cool, Ph.D.
Thesis Director

_____

Mariana Morris, Ph.D.
Department Chair

Committee on
Final Examination

_____

David R. Cool, Ph.D.

_____

James Lucot, Ph.D.

_____

Courtney E.W. Sulentic, Ph.D.

_____

Thomas Brown, Ph.D.

_____

Joseph F. Thomas, Jr., Ph.D.
Dean, School of Graduate Studies

ABSTRACT

Davidson, Molly Elizabeth. M.S., Department of Pharmacology & Toxicology, Wright State University, 2007. Neurodegeneration and Neuroinflammation in a Mouse Model of Sarin Exposure.

Sarin is an organophosphorus (OP) ester chemical warfare agent (CWA) that has been used in past terrorist attacks. It remains a threat today because of its ease of manufacture and dispersal. Sarin acts by irreversibly inactivating acetylcholinesterase and interfering with neurotransmission by allowing acetylcholine to build up at neuro-effector junctions, where it continuously elicits a response. Symptoms of sarin toxicity include seizures, hypersecretions, respiratory distress and death in extreme cases. Previous studies on OP poisoning indicate that sarin exposure causes neurodegeneration and neuroinflammation in conjunction with seizure activity. In order to determine the mode of neuronal death and the extent of neuroinflammation induced by sarin exposure, C57Bl/6J mice were first dosed s.c. with 1.5 mg/kg cresylbenzodioxaphosphorin oxide (CBDP) to inhibit the large amount of carboxylesterase found in rodents. One hour later, mice were dosed with 24 μg/kg sarin, a dose which produces approximately 17% lethality. One group of mice was also dosed with 1.7 mg/kg 8-hydroxy-2-(di-*n*-propylamino)tetralin (8-OH-DPAT), a 5-HT_{1A} receptor agonist, which has been shown by others to decrease different types of neuronal injury. Mice were sacrificed at times

ranging from four hours to ten days after sarin administration and left or right brain hemispheres were collected and frozen in isopentane for histological examination. To detect DNA fragmentation, 10μm-thick sections were TUNEL-stained using the NeuroTACS II *in situ* apoptosis detection kit. Activated caspase-3 and interleukin-1β (IL-1β) were detected by immunohistochemistry to determine whether apoptotic cell death and neuroinflammation were occurring. Manual cell counts were performed on micrographs of dentate gyrus and CA1 regions of hippocampus, amygdala and piriform cortex in NIH Image. Statistically significant TUNEL labeling was observed at various time points in all brain regions except CA1 hippocampus. Significant increases in caspase-3 staining were observed only in piriform cortex and CA1 hippocampus at 24 hours and four days post-sarin injection, respectively. IL-1β expression was significantly increased in CA1 hippocampus at four days after sarin injection and in all brain regions except piriform cortex at ten days after sarin exposure. Neither TUNEL nor caspase-3 labeling were significantly decreased with 8-OH-DPAT treatment. The amygdala and dentate gyrus regions showed significant decreases in IL-1β expression after 8-OH-DPAT treatment. Statistically non-significant upward trends over time in TUNEL labeling and IL-1β expression were observed. In contrast, caspase-3 expression exhibited a gradual, non-significant decrease at later time points. These trends may be indicative of a decreasing role played by apoptotic cell death and an increasing or persisting role for oncotic cell death and inflammation in sarin neurotoxicity.

TABLE OF CONTENTS

Page

TABLE OF CONTENTS (Continued)

Page

LIST OF FIGURES

LIST OF FIGURES (Continued)

Figure Page

LIST OF ABBREVIATIONS

5-HT_{1A}, 5-hydroxytryptamine$_{1A}$, serotonin$_{1A}$

8-OH-DPAT, 8-hydroxy-2-(di-*n*-propylamino)tetralin

AAALAC, Association for Assessment and Accreditation of Laboratory Animal Care

ACh, acetylcholine

AChE, acetylcholinesterase

CBDP, cresylbenzodioxaphosphorin oxide

CNS, central nervous system

COX-2, cyclooxygenase-2

CWA, chemical warfare agent

ER, endoplasmic reticulum

FJ-C, Fluoro-Jade C

GB, Sarin

GFAP, glial fibrillary acidic protein

IL-1β, interleukin-1 beta

IL-6, interleukin-6

IL-10, interleukin-10

JNK, jun N-terminal kinase

NATO, North Atlantic Treaty Organisation

NMDA, N-methyl-D-aspartate

OP, organophosphorus

PARP, poly-ADP ribose polymerase

PNS, peripheral nervous system

TNF-α, tumor necrosis factor alpha

TUNEL, terminal deoxynucleotidyl transferase-mediated biotinylated UTP nick end labeling

UPR, unfolded protein response

APPENDIX TABLES

LIST OF TABLES

Table Page

ACKNOWLEDGEMENT

I would like to thank everyone who has lent support, academic or otherwise, as I have pursued this degree. Without your encouragement, love and support I would not have been able to attain this honor. Thank you very much.

STATEMENT OF THE PROBLEM

A growing body of evidence indicates that sarin exposure causes neurotoxic responses including neuronal death and inflammation. An understanding of the mechanisms of sarin toxicity and development of new therapeutics for protection against the resultant damage are of great importance for the protection of soldiers and the general population in the event of a terrorist attack using organophosphates. This study employs a C57BL/6J mouse model dosed with cresylbenzodioxaphosphorin oxide (CBDP) to inhibit the endogenously high carboxylesterase activity which is common among rodents. These mice were then given a single injection of sarin. The mice were euthanized 4 hours to 10 days (240 hours) following sarin exposure and brain tissue was collected for histo-pathological staining to answer the following three questions: what is the extent of 1) neurodegeneration and cell death and 2) neuro-inflammation in this model of sarin toxicity?, and 3) does 8-OH-DPAT provide a potential therapeutic option in the event of sarin exposure?

I. INTRODUCTION

THE HISTORY OF SARIN

Sarin is an organophosphorus (OP) ester that irreversibly inhibits acetylcholinesterase (AChE). Sarin (O-isopropyl methylphosphonofluoridate) was used as a chemical warfare agent (CWA) by Iraq during the Gulf War and is a continuing terrorist threat in the current global climate. Sarin, whose NATO designation is GB, is

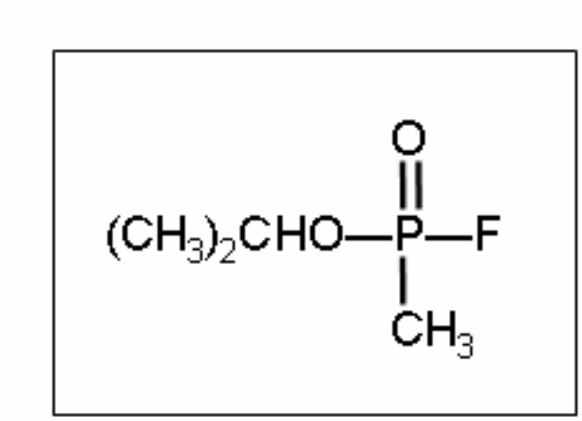

FIGURE 1. Chemical Structure of Sarin (O-isopropyl methylphosphonofluoridate):

Sarin is a colorless, odorless liquid that readily evaporates at room temperature. Exposure can occur by ingestion, inhalation of vapors, or by cutaneous contact with the liquid. All three routes of exposure can result in symptoms of sarin toxicity.

one member of a group of nerve agents that includes tabun, soman, VX and CMPF. Originally synthesized during the 1930s and 1940s by German scientists, these agents were developed as chemical weapons during WWII (Agency for Toxic Substances and Disease Registry, 2003). Sarin is a colorless, odorless liquid that can elicit toxic effects following cutaneous exposure, ingestion and/or inhalation of vapors (see Figure 1 for chemical structure). The dangerous potential of this agent was realized in June 1994 in an attack in Matsumoto, Japan and again in March 1995 during the sarin subway attack in Tokyo, Japan in which twelve people were killed, fifty seriously injured, and 5500 with less severe injuries as a result of exposure to the gas (Okumura et al., 1998). Somewhat effective therapeutic regimes against sarin do exist, including prophylactic treatment and rescue treatment immediately following exposure. However, use of these therapies is problematic, as prophylactic treatments must be given prior to exposure and the rescue treatments must be administered very quickly after exposure and before the onset of severe symptoms in order to be effective. The current treatment regime is three-fold involving 1) decontamination of victims to eliminate further exposure to the agent; 2) respiratory support to prevent lung failure as necessary; and 3) pharmaceutical treatment with an oxime to prevent permanent binding of AChE by the agent and an anti-epileptic drug to prevent neural damage as a result of seizures (Tokuda et al., 2006). The threat of terrorist activity in volatile countries coupled with the ease of manufacture and unsophisticated release of sarin highlights the need for the development of therapeutics that can be used prophylactically or as rescue treatments to prevent or decrease the damage caused in the event of an OP CWA attack.

EFFECTS OF SARIN EXPOSURE

Sarin irreversibly inhibits acetylcholinesterase (AChE), the enzyme responsible for degrading acetylcholine (ACh). The mechanism for this action is sarin binding to the serine residue within the active motif of AChE. Once bound, sarin is dealkylated leaving behind a phosphate group that cannot be removed. Most of the clinical signs and symptoms of sarin poisoning occur as a result of this AChE inhibition and the subsequent accumulation of ACh at neuroeffector junctions. ACh is a neurotransmitter that is active throughout both the central and peripheral nervous systems (CNS and PNS). ACh is responsible for synaptic transmission at autonomic parasympathetic and sympathetic neuroeffectors in addition to somatic neuroeffectors. As a result of its wide-ranging influence, interference with proper ACh function has very important physiological consequences. When released from a pre-synaptic nerve terminal ACh moves across the synapse in vesicles to the post-synaptic nerve where it is released from the vesicle, binds cholinergic receptors, is quickly released, and then hydrolyzed by AChE, which effectively inactivates the neurotransmitter (Figure 2). However, when AChE is inhibited, as in the case of OP poisoning, the ACh remains at the nerve terminal continuously binding receptors and eliciting a response from the post-synaptic nerve. Seizures, convulsions, and brain damage resembling status epilepticus are the acute symptoms of this hyper-stimulation (Hoskins et al., 1986; Gupta et al., 1987; McLean et al., 1992). More severe symptoms include respiratory distress, paralysis and coma. If these symptoms are not treated quickly they can be fatal. The therapeutic window for sarin treatment is limited due to the irreversible inhibition of AChE within approximately

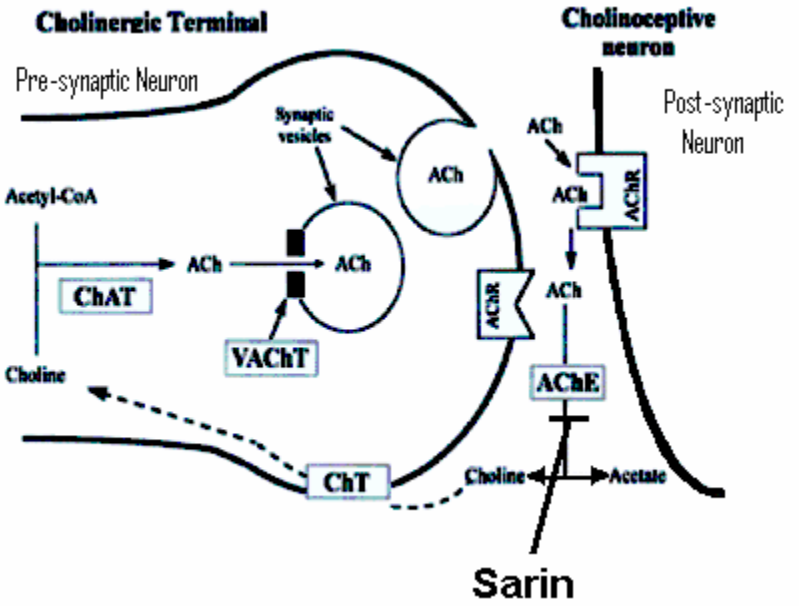

FIGURE 2. Cholinergic Synaptic Transmission: Acetylcholine is synthesized within the pre-synaptic nerve from acetate and choline, then packaged in vesicles. Upon Ca^{2+} influx into the pre-synaptic nerve, the vesicles are exocytosed and travel across the synapse to the post-synaptic nerve where ACh is released, binds cholinergic receptors, elicits a response and is then quickly released. Normally, AChE very quickly hydrolyzes ACh into its original components, which are continuously recycled. However, sarin irreversibly binds AChE, preventing the enzyme from hydrolyzing ACh in the synaptic cleft. The neurotransmitter continues to elicit a response from the post-synaptic nerve, causing seizures, convulsions, respiratory distress, neuronal damage, and possibly death if left untreated.

45 minutes of exposure. The brain regions most affected by sarin exposure are those involved in seizure activity including the hippocampus, amygdala and piriform cortex.

PROLONGED EFFECTS OF SARIN EXPOSURE

In addition to the acute symptoms, longer periods of seizure activity, due to extended exposure, exposure to high concentrations of sarin, and/or lack of therapeutic intervention, have been correlated with increased brain damage in animal models (Tanaka et al., 1996). For example, Chapman and colleagues (2006) studied the expression of inflammatory cytokines IL-1β, IL-6, TNF-α and prostaglandin E_2 in conjunction with length of sarin-induced seizure activity. Their work showed that early treatment with midazolam (an anti-epileptic drug) during seizures can decrease the amount of inflammatory cytokines found in the tissue in a time-dependent manner. Additionally, an increased presence of proinflammatory cytokines, activated astrocytes and microglia, and dead or dying neurons have been noted in animals exposed to sarin and other OPs (Henderson et al., 2002; Svensson et al., 2001; Williams et al., 2003; Chapman et al.,2006). Henderson and coworkers observed a correlation between increasing inflammatory cytokine mRNA levels (IL-1β, TNF-α, and IL-6) and higher doses of sarin in their study on rats (2002). The presence of these inflammatory factors implies that there may be additional mechanisms of toxicity, or that the toxicity of the AChE inhibition is potentiated by neuroinflammation. Furthermore, neurodegeneration and cell death have been observed in animals exposed to sarin and other OPs. Fluoro-Jade positive neurons have been detected in the brain tissue of animals exposed to sarin and other nerve agents, but this stain is nonspecific in regard to the type of cell death (i.e.

oncosis vs. apoptosis) (Carlson and Ehrich, 2004). Further exploration is necessary in order to determine what mode of cell death is occurring as a result of exposure to nerve agents. It is worthwhile to pursue these potential contributors to the toxicity of OPs since the elucidation of specific and/or additional mechanisms may lead to the discovery of more effective therapies.

MECHANISMS OF CELL DEATH

Previous animal studies of OP exposure have shown indications of neuronal cell death resulting from nerve agent toxicity. For example, a genomic study on rats performed by Damodaran and colleagues showed an increase in the production of caspase-6 and proapoptotic Bcl2lll (a member of the Bcl family) mRNA at only 2 hours following sarin exposure (2006). The early up-regulation of these genes indicates that apoptosis may indeed be a downstream result of sarin toxicity. There are two main forms of cell death: apoptosis and oncosis. Apoptosis is a carefully regulated process that, once triggered, follows a very specific and orderly cascade. Apoptosis has recently been lumped together with three additional forms of actively regulated cell death; autophagic cell death, paraptosis and programmed necrosis (reviewed by Fietta, 2006). Apoptosis and oncosis are morphologically different processes (Figure 3). The differences between apoptosis and oncosis can be observed microscopically. Apoptosis is characterized by shrinkage of the cell, plasma membrane blebbing, dismantling of the cytoskeleton, chromatin condensation and cleavage of DNA into segments of multiples of 180bp in length. In the final stages of apoptosis, the cellular contents are packaged into apoptotic

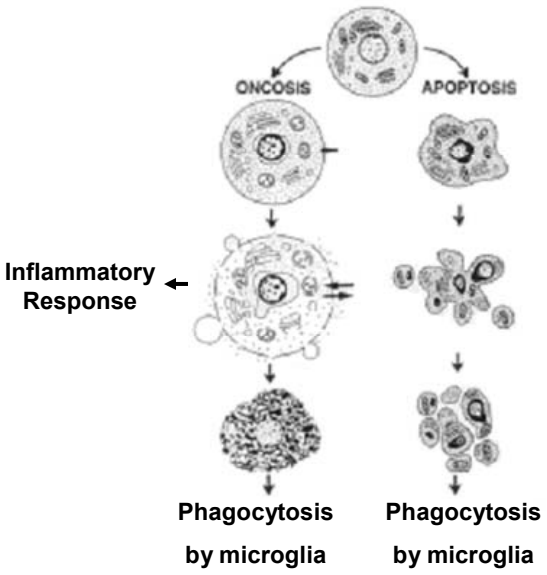

FIGURE 3. Morphological Features of Oncotic and Apoptotic Cell Death: Oncotic cells can be identified by their loss of membrane integrity, blebbing, swelling, mitochondrial shrinkage, and destruction of DNA. Apoptotic cells, on the other hand, maintain membrane integrity, shrink in size, undergo orderly cleavage of DNA, and form enclosed apoptotic bodies which then are phagocytized by neighboring microglia without the induction of an inflammatory response.

bodies which are then phagocytized by neighboring macrophages (microglia within neuronal tissue) (Wyllie, 1997). The apoptotic process is very precise and does not often interfere with the condition of neighboring cells (Wyllie, 1981). In contrast, oncosis can induce an inflammatory reaction as a result of leakage of proinflammatory cytokines into the extracellular space (Wyllie, 1997). Oncosis is characterized by the following features: loss of plasma membrane integrity and leakage of cellular contents, cytoplasmic expansion, swelling of the endoplasmic reticulum, shrinkage of mitochondria, clumping of nuclear chromatin and disorderly destruction of DNA (Majno and Joris, 1995). In addition to the microscopically observable characteristics of these two forms of cell death, there are also molecular traits that can be used to distinguish between apoptosis and oncosis. Apoptosis has been identified by the presence of cleaved poly-ADP ribose polymerase (PARP), activated forms of the effector caspases (3, 6 and 7), the appearance of a DNA ladder in gel electrophoresis, terminal deoxynucleotidyl transferase-mediated biotinylated UTP nick end labeling (TUNEL), and numerous other molecular techniques. However, most of the techniques listed above are not unique to apoptosis or oncosis, therefore it is necessary to use complimentary methods to assess the type of death undergone by cells. Caspases are the exception to this rule, as they act as the initiators and effectors of apoptosis, and are not active during oncosis. This makes them an excellent marker for the identification of apoptotic cells. Caspases are cysteine proteases that cleave proteins after aspartic acid; they are present as inactive zymogens (procaspases) in all cells, and become activated when they are cleaved into smaller subunits. The apoptotic process is carried out by a cascade of caspases, which begins with either an external or internal trigger for the initiation of cell death (Figure 4).

Externally, cell death is initiated by the extracellular binding of a cell death ligand to a death receptor on the surface of the cell. This membrane-bound receptor's internal death domain then activates caspase-8, thus initiating the caspase cascade. Apoptosis can be initiated intrinsically by either mitochondrial dysfunction or endoplasmic reticulum (ER) stress. Upon mitochondrial dysfunction there is a release of cytochrome c into the cytoplasm. This triggers Apaf-1 binding with procaspase-9, cleavage of procaspase-9 into its active form, and downstream activation of caspase-3, the first of the effector caspases to be triggered. In the event of ER stress, the unfolded protein response (UPR) is invoked in an attempt to alleviate the buildup of unfolded proteins. If ER stress continues for an extended period of time and the UPR cannot overcome it, the cell will be committed to die by apoptosis through the expression of Bax and JNK. After commitment there is downstream formation of the apoptosome complex and a parallel induction of the mitochondrial apoptosis pathway by cytochrome c release (Smith and Deshmukh, 2007). The extrinsic and intrinsic pathways converge at caspase-3, making this an ideal biomarker to determine whether or not apoptosis is occurring, regardless of the initial trigger for death. TUNEL labeling in conjunction with detection of activated caspase-3 provides sufficient evidence of apoptosis. This study will focus on the presence of apoptotic cell death and inflammation occurring in the brains of mice exposed to sarin.

EFFECTORS AND MARKERS OF THE NEUROINFLAMMATORY RESPONSE

Microglia are the primary immune cells within the brain and act as phagocytes to remove the debris when neighboring cells die. Microglia are also responsible for the

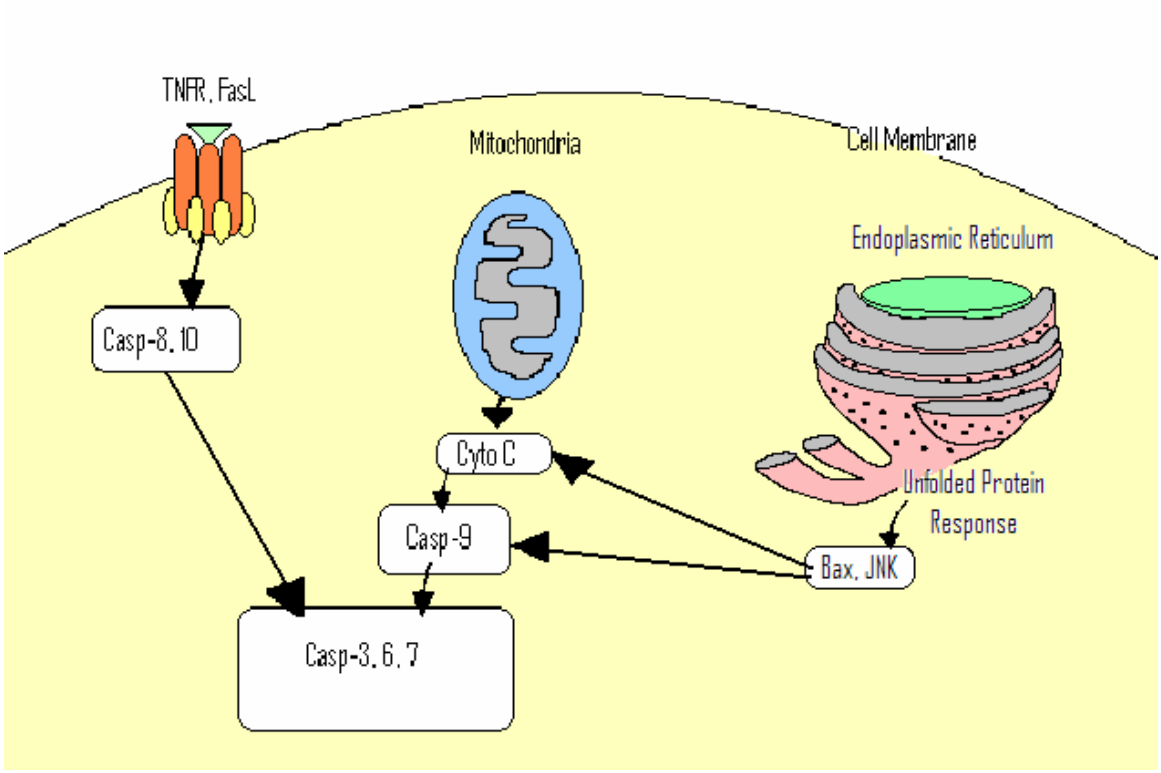

FIGURE 4. Extrinsic and Intrinsic Apoptotic Pathways: Apoptosis can be initiated extrinsically by binding of a death ligand to a membrane-bound death receptor (i.e. Fas ligand and TNF receptor.) Within the cell, apoptosis can be initiated by mitochondrial release of cytochrome c, or by persistent ER stress and subsequent activation of Bax and JNK. All three initiators trigger activation of caspases, the effectors of apoptosis.

initiation of the neuroinflammatory response. When activated, microglia release IL-1α, IL-1β and TNF-α, thus initiating the cytokine cascade (McGeer and McGeer, 1995). In addition to the proinflammatory cytokines released by activated microglia, they also contribute enzymes that help carry out the inflammatory process (Wood, 2003). Under normal conditions, the inflammatory process provides essential housekeeping activities, but when neuroinflammation persists, cytokines, chemokines, enzymes and reactive oxygen species can create a toxic environment for neurons (Wood, 2003). Once the inflammatory cascade has been initiated by microglia, astrocytes are recruited and begin releasing their own inflammatory signals, further contributing to the unhealthy environment and leading to neuronal damage (Davies et al., 1999; Svensson et al., 2001) (Figure 5).

There are many examples of correlations between seizure activity and presence of inflammatory markers in the brain. For instance, in a study performed on rats by Steward and coworkers (1991) electrically induced seizures caused an increase in glial fibrillary acidic protein (GFAP) mRNA expression, indicative of activated astrocytes resulting from inflammation in brain and post-synaptic regions stimulated by the seizure activity. In addition, Damodaran and colleagues observed up-regulation of GFAP and IL-10 mRNA in a rat model two hours after exposure to sarin, suggesting the presence of an early inflammatory response accompanied by an anti-inflammatory counteraction (2006). Similarly, Tu and Bazan (2003) noted an increase in neuronal COX-2 expression, which plays an important role in inflammation, in their model of hippocampal kindling (based on the premise that repeated induction of low-intensity seizures decreases the threshold for induction of future seizures). These studies indicate that excessive brain stimulation

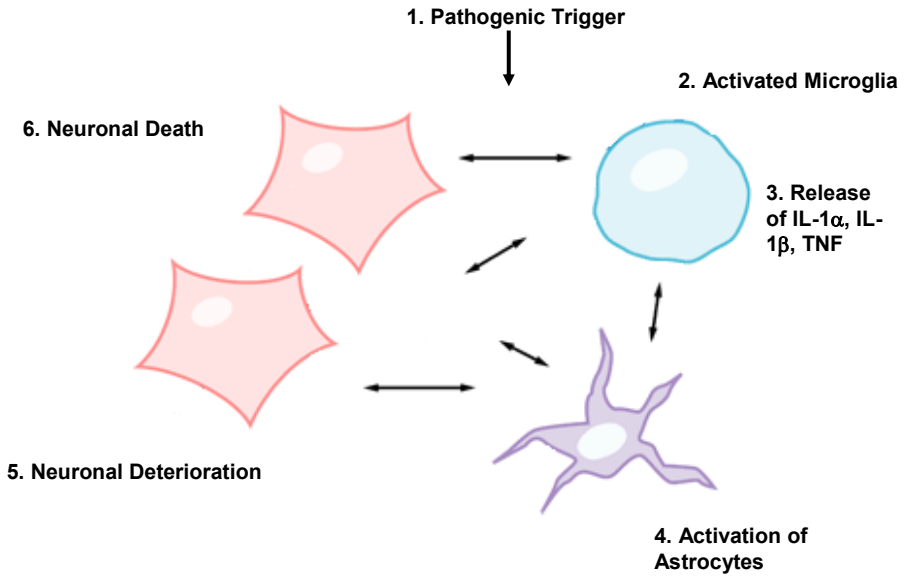

FIGURE 5. Neural Inflammatory Response: Microglia initiate the neuroinflammatory response by releasing proinflammatory cytokines (i.e. IL-1α, IL-1β and TNF.) These proinflammatory signals then trigger activation of astrocytes, which begin releasing additional inflammatory signals. Prolonged neuroinflammation creates a toxic environment for neurons eventually leading to degeneration and death.

initiates inflammatory processes. Additionally, Zimmer and colleagues (1997) found that seizures caused by soman increased the presence of activated astrocytes and microglia in several brain regions including the piriform cortex, amygdala and hippocampus. It follows that sarin-induced seizures may also cause neuroinflammation as a result of overstimulation of specific brain regions, and that this inflammatory activity may cause ancillary damage to surrounding neurons, thus having a long-lasting impact on brain function.

IL-1β is an effective biomarker for inflammation. According to a 2004 study by Basu and colleagues, blocking IL-1 activity with a receptor antagonist effectively reduces the amount of neuronal damage that occurs as a result of stroke. This is significant because a great deal of the brain damage associated with stroke occurs as a result of reperfusion toxicity and the ensuing inflammatory response (Basu, et al., 2005). The role of microglia as the only resident immune cells within the brain and as the initiators of the inflammatory response therein indicates that their early release of IL-1β is one of the very first steps in the inflammatory cascade. Therefore, the presence of IL-1β in the brain tissue of an animal model is indicative of an ongoing inflammatory response within that tissue.

POTENTIAL THERAPY: SEROTONIN$_{1A}$ AGONIST 8-OH-DPAT

Serotonin$_{1A}$ (5-HT$_{1A}$) receptors are localized in brain regions that are particularly susceptible to excitotoxic injury, including hippocampus and cortex (Chalmers and Watson, 1991; Nyakas et al., 1997). The 5-HT$_{1A}$ receptor is G_i protein-linked and once activated triggers an intracellular signaling pathway (Fargin et al., 1989). Activation of

the 5-HT_{1A} receptor is capable of affecting adenylyl cyclase activity, increasing hydrolysis of phosphoinositol and increasing potassium ion conductance in different experimental models (Fargin et al., 1989). Therapeutic use of agonists of the 5-HT_{1A} receptor have been reported to decrease the damage caused by different types of neuronal injury including ischemia, traumatic brain injury and NMDA-induced excitotoxicity (Ramos et al., 2004; Kline et al., 2001; Ohman et al., 2001; Oosterink et al., 2003). Although the exact mechanism of attenuation of neuronal damage by 5-HT_{1A} receptor agonists is currently unknown, it has been hypothesized that it occurs because of a decrease in intracellular Ca^{2+} (Colino and Halliwell, 1987; Liu and Albert, 1991; Prehn et al., 1993). This hyperpolarization of neurons decreases their capacity to fire, hence attenuating seizure activity and the subsequent neuronal damage. Another potential mechanism of action is the inhibition of glutamate release by the activation of 5-HT_{1A} receptors (Srkalovic et al., 1994.) Glutamate is the primary excitatory amino acid in the brain. It is responsible for the continuous activation of NMDA receptors that initiates excitotoxicity. A third possible mechanism of 5-HT_{1A} receptor agonists is the activation of the MEK/ERK signaling pathway. Adayev and colleagues (1999) proposed that the activation of the MEK/ERK signaling pathway through 5-HT_{1A} receptors could prevent the activation of caspase-3, thereby inhibiting apoptosis, one of the potential endpoints of neurotoxicity. The mechanism proposed by Adayev may account for a decrease in cell death resulting from excitotoxicity, but it does not explain a decrease in the neuroinflammatory response. Based on the known link between seizure activity and the induction of an inflammatory response, the two former explanations (neuronal hyperpolarization and attenuation of glutamate release) could account for a decrease in

inflammation as a result of 5-HT_{1A} agonism. The drug 8-hydroxy-2-(di-*n*-propylamino)tetralin (8-OH-DPAT) is a selective agonist of the 5-HT_{1A} receptor. This drug has been shown to decrease neuronal death *in vitro* under anoxic conditions and *in vivo* under excitotoxic conditions (Adayev et al., 1999; Oosterink et al., 2003). In addition, 8-OH-DPAT decreased neuronal death and neuroinflammation *in vivo* following ischemic brain damage in a rat model (Ramos et al., 2004.) The current study will examine the effectiveness of 8-OH-DPAT against inflammation and apoptotic cell death in the brains of mice exposed to a single s.c. injection of the nerve agent sarin.

CARBOXYLESTERASE SCAVENGER: CBDP

Rodents have a great deal of carboxylesterase that inactivates OPs before they can interact with AChE to produce the classical symptoms of OP poisoning. Cresylbenzo-dioxaphosphorin oxide (CBDP) is a carboxylesterase inhibitor. CBDP scavenges excess rodent carboxylesterase and effectively increases the animals' susceptibility to OP poisoning, making their exposure at low doses more representative of human exposure. Application of CBDP decreases cross-species variability in the LD_{50} of sarin from 22.8-125 μg/kg to 11.8-15.6 μg/kg (Maxwell et al., 1987). Preliminary work has shown that a dose of 1.5 mg/kg CBDP does not cause toxicity alone, and potentiates the response of C57BL/6J mice to sarin.

HYPOTHESIS

The large body of evidence indicating that neuroinflammation and neurodegeneration are symptoms of sarin exposure and the relatively novel concept that

5-HT_{1A} agonists are potentially useful at decreasing damage due to excitotoxicity lead to the development of the following hypothesis: exposure of mice to sublethal doses of sarin causes apoptosis and inflammation in brain regions susceptible to excitotoxicity; i.e., piriform cortex, amygdala and hippocampus. These neuropathologic conditions can be attenuated by treatment with 8-OH-DPAT, a 5-HT_{1A} receptor agonist. The objective of this study was two-fold: 1) to confirm that neurodegeneration and neuroinflammation occur in our model of sarin toxicity, which differs from other models in the use of CBDP as a carboxylesterase inhibitor; and 2) to determine whether these toxic responses could be attenuated by therapeutic use of a 5-HT_{1A} receptor agonist. These two objectives were divided based on the symptoms to be examined (i.e. neurodegeneration and neuroinflammation) into two specific aims.

SPECIFIC AIM 1

Test the hypothesis that sarin induces apoptosis in the piriform cortex, amygdala, dentate gyrus and CA1 region of hippocampus, and that this neurodegeneration can be attenuated by a therapeutic dose of 8-OH-DPAT.

SPECIFIC AIM 2

Test the hypothesis that sarin induces an inflammatory response in the piriform cortex, amygdala, dentate gyrus and CA1 region of hippocampus, and that the neuroinflammation can be attenuated by a therapeutic dose of 8-OH-DPAT.

II. MATERIALS & METHODS

DRUGS

CBDP was delivered in propylene glycol and 5% ethanol at a concentration of 0.15mg/mL. Mice were dosed with 1.5 mg/kg CBDP 1 hour prior to receiving a dose of sarin. Sarin was diluted from a stock of 1.9 mg/mL in saline solution (original stock obtained from Aberdeen Proving Ground, MD). Sarin was injected in a volume of 1 mL/100 g weight to obtain a dose of 24µg/kg. 8-OH-DPAT (Sigma, St. Louis, MO) was dissolved in 0.9% saline and given at a dose of 1.7mg/kg 1 minute after sarin injection. All injections were subcutaneous (s.c.).

ANIMALS

Male C57BL/6J mice at 20-25g body weight were used in this study. The mice were housed in an AAALAC (Association for the Assessment and Accreditation of Laboratory Animal Care) approved facility on a 12 hour light/dark cycle with free access to food and water. Six groups of mice received different treatments: Group 1, the negative control group received propylene glycol and saline (vehicles for CBDP and sarin, respectively) and were euthanized four or ten days (240 hours) after injection; Groups 2, 3, 4 and 5 received CBDP and sarin and were euthanized four, 24, 96 and 240 hours after injection, respectively; and Group 6 received CBDP, sarin and 8-OH-DPAT and were euthanized 240 hours (10 days) after injection. (See Table 1 for n values of each group.)

Group	TUNEL	Caspase-3	Interleukin-1β
Negative Control	4	5	4
4 Hours Post-Sarin	2	2	2
24 Hours Post-Sarin	2	2	2
96 Hours Post-Sarin	4	9 (8 Piriform)	6
240 Hours Post-Sarin	5 (3 Amygdala)	6 (5 Amygdala)	5
240 Hours Post-Sarin/8-OH-DPAT	6	6 (5 Amygdala)	6

TABLE 1. Summary of n Values of Experimental Groups: n-values for each group and each staining technique are stated. Values were the same across all brain regions examined except where stated specifically for individual regions.

TISSUE COLLECTION AND SECTIONING

Following treatment, mice were sacrificed by decapitation after CO_2 knockout and brain tissue was collected for histology. Brains were removed and separated into left and right hemispheres. One half of each brain was quick frozen in isopentane for 30 seconds and then stored at -80°C until sectioning. Brain tissue was mounted on a cryotome chuck, covered with tissue freezing medium (Triangle Biomedical Sciences, Durham, NC), and coronally sliced on a cryotome (at approx. -20°C) at 10μm thickness throughout brain regions inclusive of amygdala, hippocampus, and piriform cortex. Sections were collected on UltraStick slides (Gold Seal Products, Portsmouth, NH) and stored at -20°C until fixed for staining.

FLUORO-JADE C STAINING

Tissue sections affixed to slides were placed in 1% NaOH/80% ethanol for 5 minutes at room temperature, then in 70% ethanol for 2 minutes Slides were rinsed in deionized water for 2 minutes. Potassium permanganate solution (0.06% in deionized water) was applied to sections for 10 minutes. Slides were then rinsed in tap water for 2 minutes. Dilute Fluoro-Jade C (0.0001% in acetic acid vehicle [Chemicon International, Temecula, CA]) was applied to sections and incubated in the dark at room temperature for 10 minutes. Sections were rinsed with deionized water 3 times, 1 minute each. Slides were allowed to dry on a slide warmer at approximately 50°C for 5 minutes, then cleared for 1 minute in HistoChoice clearing agent (Sigma, St. Louis, MO). Coverslips were mounted with DPX mounting medium (Fluka, Buchs, Switzerland) and stored in the dark until microscopic analysis.

TERMINAL DEOXYNUCLEOTIDYL TRANSFERASE-MEDIATED BIOTINYLATED UTP NICK END LABELING (TUNEL)

TUNEL staining was performed on brain sections using the NeuroTACS II *In Situ* Apoptosis Detection Kit (Trevigen, Gaithersburg, MD). The assay protocol provided by the manufacturer was followed with the addition of three steps to optimize staining. After rehydration in alcohols, lipids were extracted from the brain tissue sections by dipping slides in chloroform for 5 seconds, then incubating at room temperature for 10 minutes in methanol, followed by washing twice in 1X PBS for 5 minutes each. Next, the sections were fixed in 3.7% buffered paraformaldehyde for 10 minutes. After this step the kit protocol was followed with the exception of an additional wash after the 10 minute incubation in Strep-HRP solution. Samples were washed twice in 1X PBS containing 1% BSA and 0.05% Tween-20. The counterstaining step was omitted. Slides were allowed to dry and coverslipped with Permount (Fisher, Pittsburgh, PA) mounting medium.

CASPASE-3 IMMUNOFLUORESCENT STAINING

Prior to staining, tissue sections were fixed to glass slides by incubating for 15 minutes in 3.7% buffered paraformaldehyde. After fixation, slides were washed three times for 5 minutes in 1X PBS and blocked for 1 hr. in 10% normal horse serum (diluted in 1X PBS/0.02% Triton X-100). The primary antibody, anti-cleaved caspase-3 rabbit polyclonal antibody (Cell Signaling Technology, Boston, MA), which detects only the 17 kDa subunit of activated caspase-3, was diluted to 1:250 in 1X PBS, applied to sections, and incubated overnight at 4°C in a humid chamber. Primary antibody was removed and

sections washed as described above. The secondary antibody, Biotin-SP conjugated Donkey anti Rabbit (Jackson Immunoresearch Laboratories, West Grove, PA), was diluted 1:500 in 1X PBS and incubated on tissue-fixed slides for 1 hour at room temperature in the dark. Secondary antibody was removed and sections were washed three times for 5 minutes each in 1X PBS. The third antibody, streptavidin conjugated Cy 3, was diluted 1:200 in 1X PBS, and incubated with the tissue-fixed slides for 1 hour at room temperature in the dark. After removal of the third antibody, sections were washed as described above then incubated with 0.01 mg/mL Hoechst stain (H3569, Invitrogen, Eugene, OR) for 10 minutes at room temperature in the dark. Hoechst stain labels all nuclei and allows for the visualization of brain structures. Sections were washed in deionized water for several minutes and coverslips were mounted with Gel Mount mounting medium (Biomeda, Foster City, CA).

INTERLEUKIN-1β IMMUNOFLUORESCENT STAINING

Tissue-fixed slides were stained for IL-1β as described above for caspase-3 staining with the exception of using a primary rabbit polyclonal antibody against IL-1β, diluted 1:1000 (sc-7884 from Santa Cruz Biotechnology, Santa Cruz, CA).

IMAGE CAPTURE

All fluorescently stained sections were viewed on a Leica DMR microscope under the fluorescein isothiocyanate (FITC) filter or rhodamine filter set. Hippocampus (dentate gyrus and CA1 regions), amygdala and piriform cortex regions (Figure 6) of each TUNEL, IL-1β, or caspase-3-stained section were viewed and micrographs taken at

20X magnification using an Optronics Magnafire CCD camera with MagnaFire software v.2.0 (Optronics, Goleta, CA).

DATA/STATISTICAL ANALYSIS

Micrograph images were opened in NIH ImageJ v.1.37 and positively labeled cells within defined areas were counted using the cell counter plug-in. Areas for amygdala, piriform cortex and CA1 regions were 450µm x 450µm, while areas for dentate gyrus counts were 450µm x 275µm. In most cases, TUNEL labeling of only one section per animal was counted, whereas for caspase-3 and IL-1β, staining of two sections per animal was assessed. There were exceptions to this when sections were damaged during processing and/or brain regions were indistinguishable, preventing accurate cell counts (see Appendix for details of TUNEL, caspase-3 and IL-1β staining). Cell counts were uploaded into GraphPad Prism v.4.03 software where one-way ANOVA and Tukey-Kramer post-hoc test (with correction for groups of different sizes) were performed. P values of less than 0.05 were accepted as significant. All values are reported as mean ± standard deviation. Refer to Table 1 for n values of each experimental group.

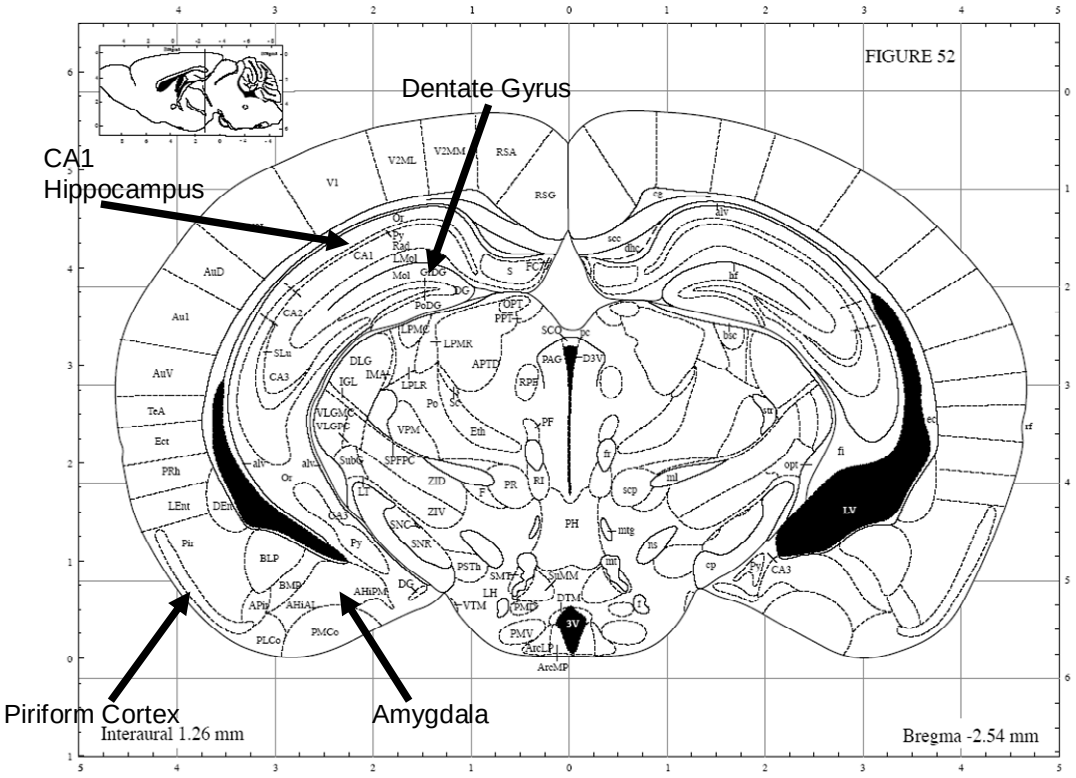

FIGURE 6. Brain Regions of Interest: Amygdala, dentate gyrus, CA1 hippocampus and piriform cortex regions were photographed under 20X magnification. Labeled cells were counted, and counts were averaged to obtain a mean value for each group.

III. RESULTS

FLUORO-JADE C STAINING

The presence of positive staining by Fluoro-Jade C is an indicator for cells undergoing neurodegeneration. Sections of brain tissue from negative control mice receiving only injections of vehicle showed virtually no specific staining, i.e., degenerating neurons (Figure 7a). When tissue sections from mice treated with sarin were stained with Fluoro-Jade C we observed a few labeled cells in the amygdala, dentate gyrus, CA1 region of hippocampus and piriform cortex (Figure 7b, c, and d). Because this staining technique was intended only to establish evidence of neurodegeneration, positively labeled cells were not quantified.

TUNEL STAINING

TUNEL staining is a method of analyzing nuclear DNA in intact cells and is used as an indicator of cell death. Based on the Fluoro-Jade C staining, we chose to examine the same four brain regions by TUNEL assay. Statistical analysis of cell counts in amygdala, dentate gyrus, CA1 hippocampus and piriform cortex of sarin treated mice showed a significant increase in the number of TUNEL-positive cells compared to negative control tissues (from animals receiving propylene glycol and saline injections) (Figure 8). Specifically, a significant increase in TUNEL-labeled cells was observed in the amygdala four days after a 24μg/kg dose of sarin ($F_{4, 10}$=4.456, $p<0.05$)(Figure 9a).

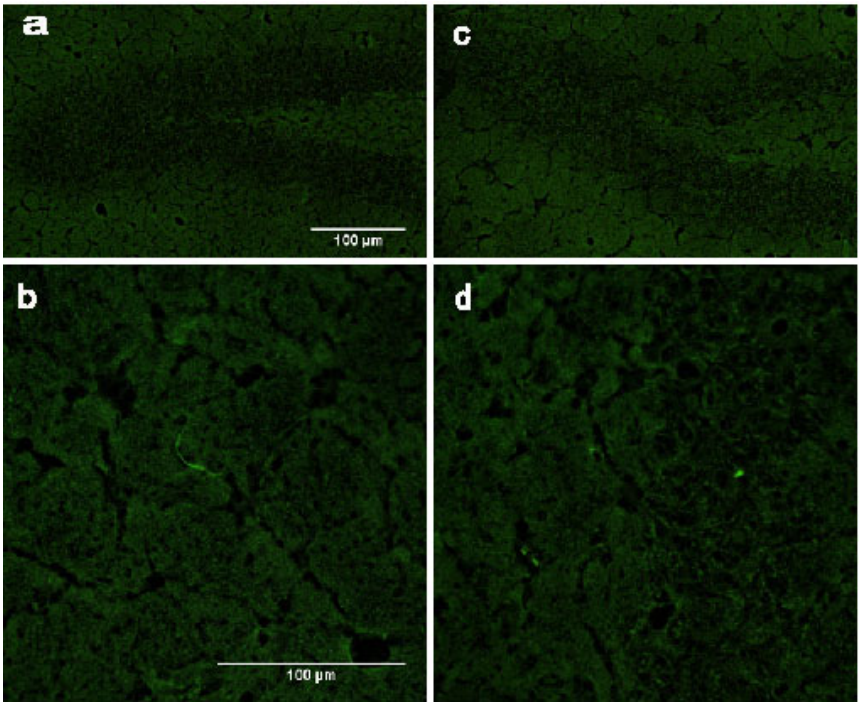

FIGURE 7. Fluoro-Jade C Staining in Mouse Brain Tissue 4 Days After Sarin Treatment: a) Dentate gyrus of a mouse treated with vehicle only at 20X magnification; b) CA2 region of a mouse given 32µg/kg sarin + 1.5mg/kg CBDP at 40X magnification; c) dentate gyrus of a mouse treated with 32µg/kg sarin + 1.5mg/kg CBDP at 20X magnification; and d) Dentate gyrus of a mouse treated with 32µg/kg sarin + 1.5mg/kg CBDP at 40X magnification. Note that there is virtually no specific staining in the negative control tissue, while some Fluoro-Jade C-positive cells can be observed in the tissue of sarin treated mice. Scale bars represent 100µm.

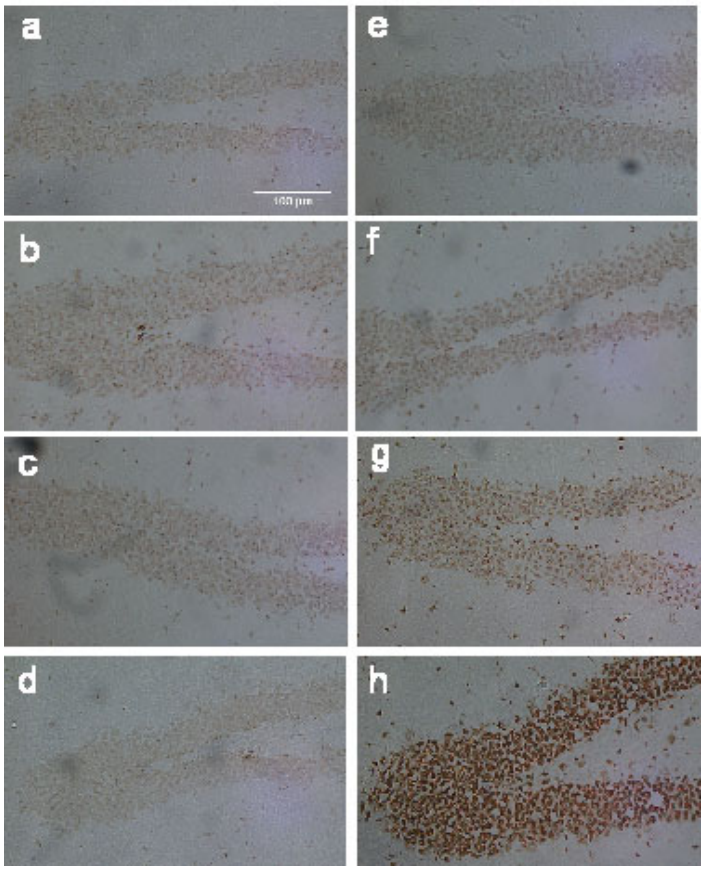

FIGURE 8. TUNEL Labeling in the Dentate Gyrus: Micrographs showing representative TUNEL-labeled brain sections from a) negative control mouse treated with vehicle only; b) mouse treated with 1.5mg/kg CBDP + saline; c), d), e), and f) mice treated with 1.5mg/kg CBDP + 24μg/kg sarin and euthanized at 4, 24, 96, and 240 hours after treatment, respectively; g) mouse treated with 1.5mg/kg CBDP + 24μg/kg sarin + 1.7mg/kg 8-OH-DPAT; and h) positive control generated using TACS nuclease. Scale bar represents 100μm. Due to the inherent issues with decreasing the size of the photomicrographs, differences between differently treated tissues are difficult to detect visually, as seen in this figure.

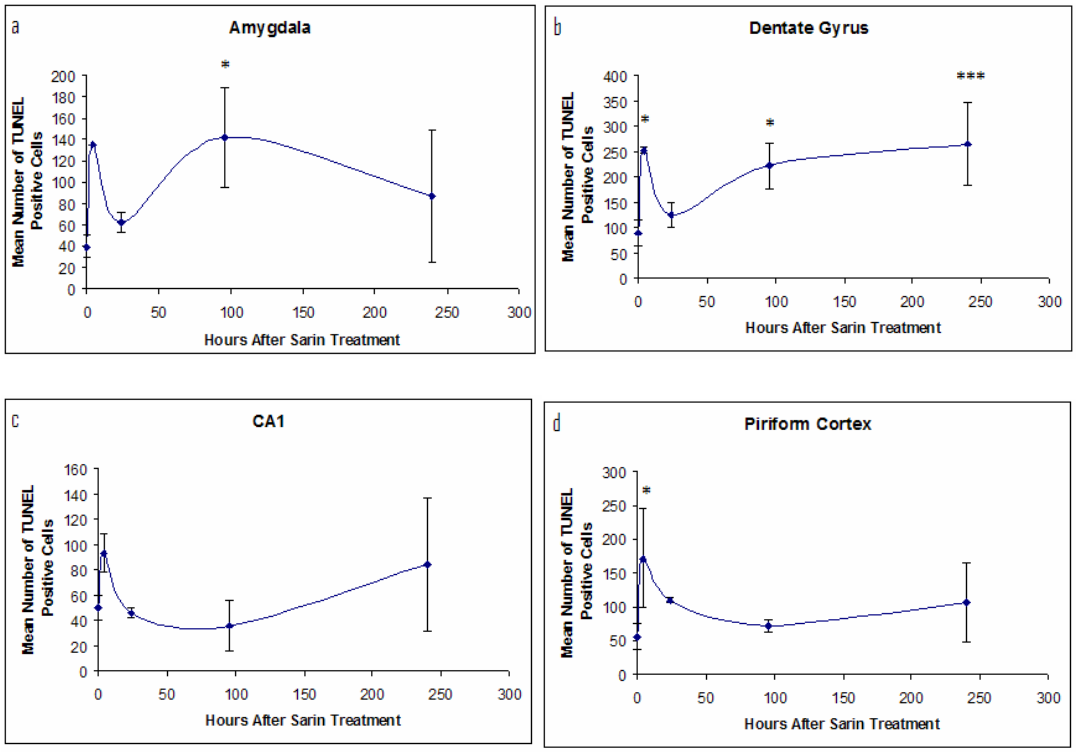

FIGURE 9. TUNEL Labeling in the amygdala, dentate gyrus, CA1 hippocampus and piriform cortex: The plotted values represent the mean number of TUNEL-positive cells ± S.D. in the (a) amygdala, (b) dentate gyrus, (c) CA1 hippocampus, and (d) piriform cortex of mice given 24µg/kg sarin at four hours, 24 hours, four days and ten days post-dose. $F_{4, 10}$=4.456 for amygdala, $F_{4, 12}$=7.488 for dentate gyrus, $F_{4, 12}$=1.963 for CA1, and $F_{4, 12}$=3.071 for piriform cortex. A p-value <0.05 was considered significant (* $p<0.05$, *** $p<0.001$).

In the piriform cortex there was a significant increase in TUNEL-positive cells only four hours after sarin treatment ($F_{4, 12}$=3.071, $p<0.05$; Figure 9d). In the dentate gyrus, there were significant increases in TUNEL staining in sarin treated mice four hours, four days, and ten days post-dose ($F_{4, 12}$=7.488, $p<0.05$; $p<0.05$; and $p<0.001$, respectively; Figures 8c, e, f, and 9b). The CA1 hippocampal region showed no significant increase in staining at any examined timepoint as a result of exposure to sarin (Figure 9c). In order to assess the efficacy of the 5-HT_{1A} agonist in preventing neuronal cell death as a result of sarin exposure, one group of mice was given a therapeutic dose of 8-OH-DPAT one minute after sarin injection. This group of mice was euthanized 10 days after injection and staining was compared with the negative control tissues and with tissues from sarin treated mice from the same timepoint. Treatment with 1.7mg/kg 8-OH-DPAT did not cause any significant decreases in TUNEL staining in any of the brain regions of interest at ten days post-dose (Figure 10).

CASPASE-3 STAINING

Caspases are cell death enzymes activated in cells destined to undergo apoptosis. In many cases, apoptosis is deliberate and necessary. In other cases, apoptosis is not part of the pre-determined order of life for the cell and is deemed inappropriate. When this occurs, the cell undergoes abnormal cell death, causing changes in the capacity of the tissue or organ to function normally. Statistical analysis of the cell counts from sections stained for the active form (17kDa subunit) of caspase-3 indicated significant increases in staining over the negative control tissues (animals receiving propylene glycol and saline injections) only in CA1 hippocampus four days after sarin injection ($F_{4,19}$=3.531, $p<0.05$)

(Figure 11c) and in piriform cortex 24 hours after sarin injection ($F_{4,18}$= 5.049, $p<0.05$) (Figure 11d). No other brain regions showed significant increases in caspase-3 activity with sarin exposure (Figure 12). Animals given a therapeutic dose of 8-OH-DPAT one minute after sarin injection and euthanized 10 days after treatment were compared with negative control and sarin treated mouse tissue from the 10 day post-sarin dose time point. No significant decrease in caspase-3 activity was observed as a result of treatment with 8-OH-DPAT, however, there were no significant increases in caspase-3 activity at the 10 day timepoint, so this result is not necessarily indicative of the effectiveness of 8-OH-DPAT treatment (Figure 13).

INTERLEUKIN-1β STAINING

IL-1β is a proinflammatory cytokine whose expression is indicative of an inflammatory response. Statistical analysis of IL-1β staining in the four brain regions of interest (Figure 14) revealed significant increases in IL-1β expression at ten days after sarin injection in amygdala, dentate gyrus and CA1 hippocampus ($F_{4,14}$= 6.625, $p<0.01$; $F_{4,14}$= 9.853, $p<0.001$; and $F_{4,14}$= 4.358, $p<0.05$, respectively) (Figure 15a, b, and c, respectively). Additionally, in the CA1 region of hippocampus, there was a significant increase in IL-1β protein four days after sarin treatment ($F_{4,14}$= 4.358, $p<0.01$). The piriform cortex had no significant changes in IL-1β expression as a result of exposure to a 24μg/kg dose of sarin (Figure 15d). The usefulness of 8-OH-DPAT treatment against the inflammatory consequences of sarin exposure was tested by comparing the mean number of IL-1β-positive cells in groups dosed with sarin plus 8-OH-DPAT, sarin alone, and propylene glycol plus saline (negative control) 10 days after injection. Comparison

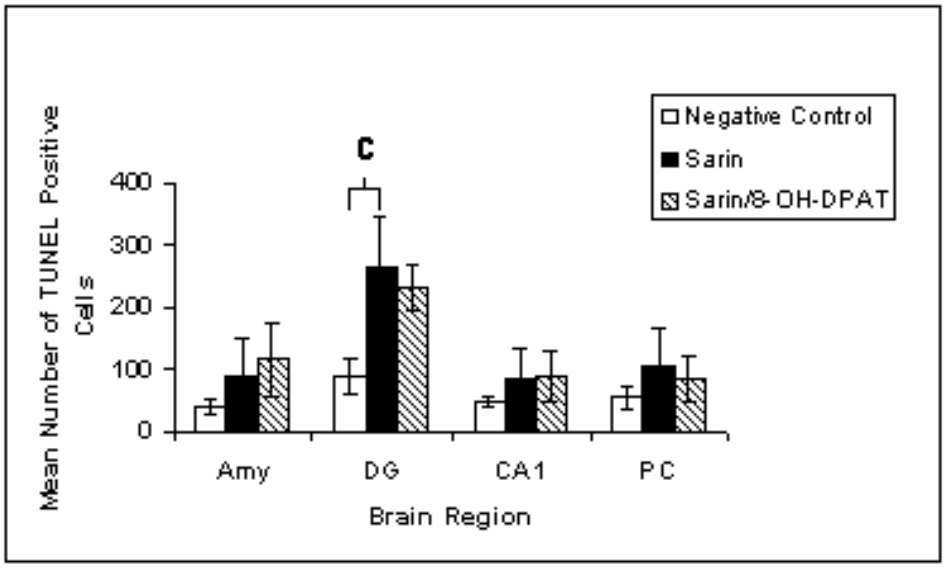

FIGURE 10. TUNEL Labeling 10 Days after Treatment with Sarin and 8-OH-DPAT: Graph showing the mean number of TUNEL-positive cells in amygdala, dentate gyrus, CA1 hippocampus and piriform cortex ten days after treatment. Negative control mice were dosed with propylene glycol and saline, sarin mice received 24μg/kg sarin, sarin/8-OH-DPAT mice received 24μg/kg sarin and 1.7mg/kg 8-OH-DPAT. Each bar represents the mean ± S.D. $F_{2, 10}$=2.736 for amygdala, $F_{2, 12}$=12.77 for dentate gyrus, $F_{2, 12}$=1.241 for CA1, $F_{2, 12}$=1.593 for piriform cortex. A p-value <0.05 was considered significant (c = $p<0.001$).

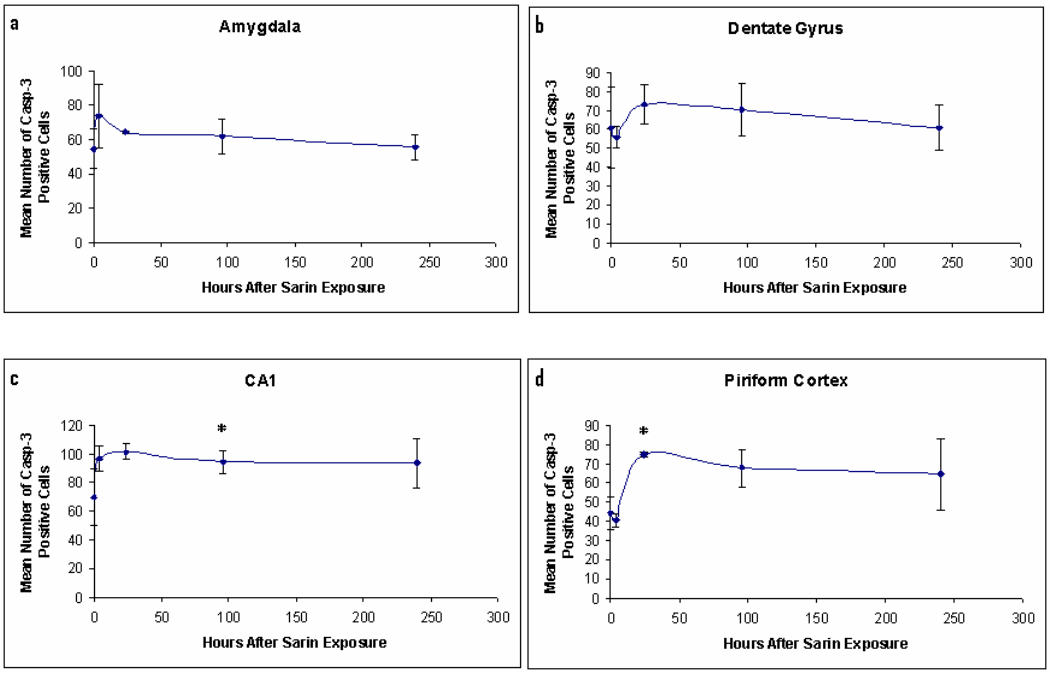

FIGURE 11. Temporal Changes in Caspase-3 Activity After 24µg/kg Sarin in Four Brain Regions: The plotted values represent the mean number of caspase-3-positive cells ± S.D. in the (a) amygdala, (b) dentate gyrus, (c) CA1 hippocampus, and (d) piriform cortex of mice given 24µg/kg sarin at four hours, 24 hours, four days and ten days post-dose. $F_{4,18}$= 1.639 for amygdala, $F_{4,19}$= 0.8717 for dentate gyrus, $F_{4,19}$=3.531 for CA1, and $F_{4,18}$= 5.049 for piriform cortex. A p-value <0.05 was considered significant (* $p<0.05$).

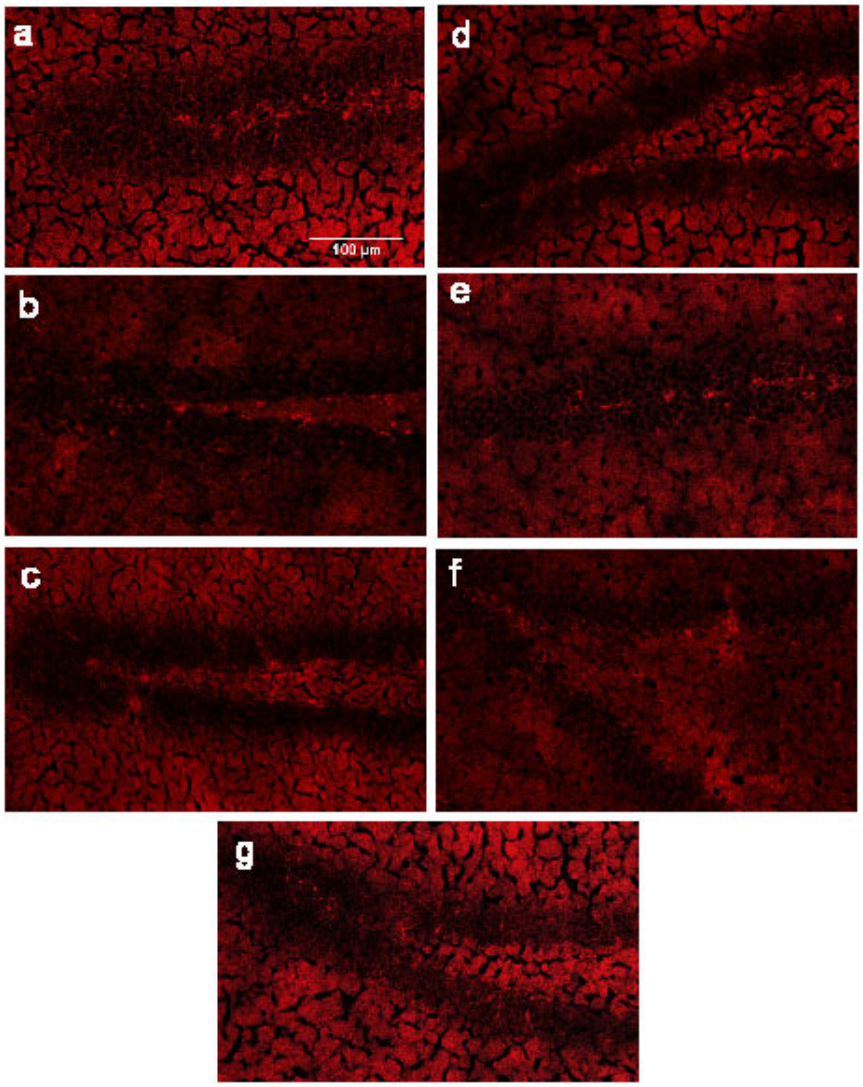

FIGURE 12. Caspase-3 Staining in the Dentate Gyrus: Micrographs showing a) negative control mouse tissue treated with propylene glycol and saline; b) tissue from a mouse treated with 1.5mg/kg CBDP and euthanized 96 hours after treatment; c); d); e); and f) tissue from mice treated with 1.5mg/kg CBDP + 24µg/kg sarin and euthanized 4, 24, 96, and 240 hours after injection, respectively; and g) tissue from a mouse treated with 1.5mg/kg CBDP + 24µg/kg sarin + 1.7 mg/kg 8-OH-DPAT. Scale bar represents 100µm.

As in Figure 8, due to the inherent issues with decreasing the size of the photo-micrographs, differences in staining between differently treated tissues are difficult to detect visually.

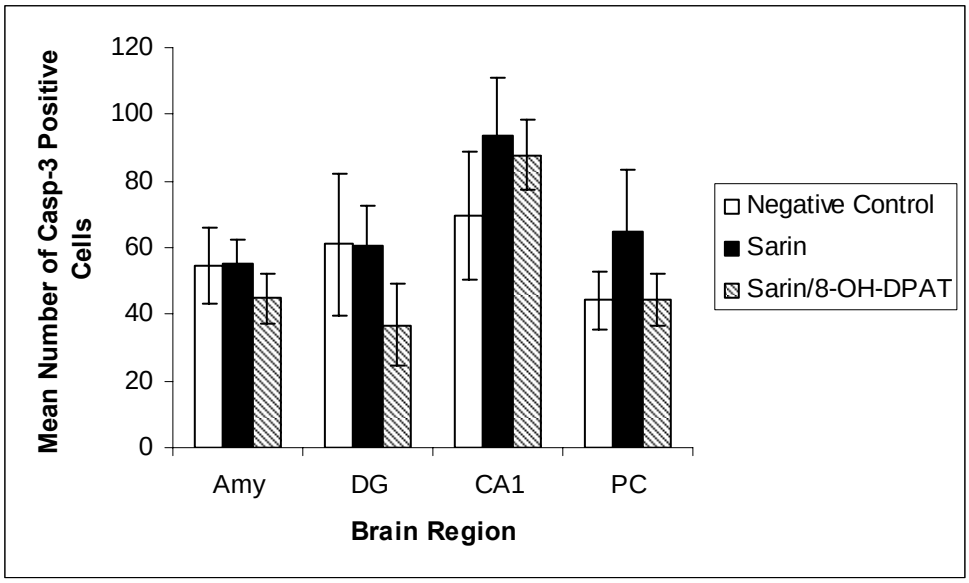

FIGURE 13. Caspase-3 Staining 10 Days after Treatment with Sarin and 8-OH-DPAT: Graph showing the mean number of caspase-3-positive cells in amygdala, dentate gyrus, CA1 hippocampus and piriform cortex ten days after treatment. Negative control mice were dosed with propylene glycol and saline, sarin mice received 24μg/kg sarin, sarin/8-OH-DPAT mice received 24μg/kg sarin and 1.7mg/kg 8-OH-DPAT. Each bar represents the mean ± S.D. $F_{2,12}$= 2.302 for amygdala, $F_{2,14}$= 4.684 for dentate gyrus, $F_{2,14}$= 3.253 for CA1, and $F_{2,14}$= 4.783 for piriform cortex. A p-value <0.05 was considered significant.

of the means of each group at the ten day timepoint showed a significant decrease in IL-1β staining in the amygdala ($F_{2,12}$= 17.27, $p<0.05$) and in the dentate gyrus ($F_{2,12}$= 18.44, $p<0.01$) of animals that received a dose of 8-OH-DPAT one minute after the sarin injection (Figure 16).

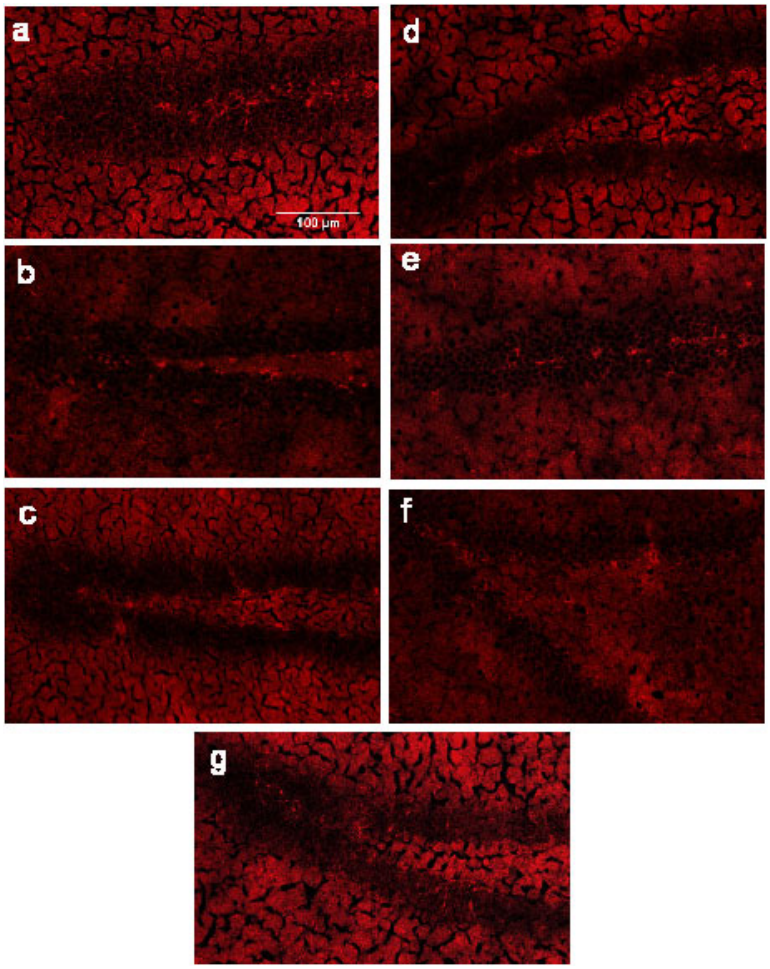

FIGURE 14. IL-1β Staining in the Dentate Gyrus: Micrographs showing a) negative control mouse tissue treated with propylene glycol and saline vehicles; b) brain tissue from a mouse treated with 1.5mg/kg CBDP and euthanized 96 hours after treatment; c); d); e); and f) tissue from mice treated with 1.5mg/kg CBDP + 24µg/kg sarin and euthanized 4, 24, 96, and 240 hours after injection, respectively; and g) tissue from a mouse treated with 1.5mg/kg CBDP + 24µg/kg sarin + 1.7 mg/kg 8-OH-DPAT. Scale bar represents 100µm. As in Figure 8, due to the inherent issues with decreasing the size

of the photomicrographs, differences in staining between differently treated tissues are difficult to detect visually.

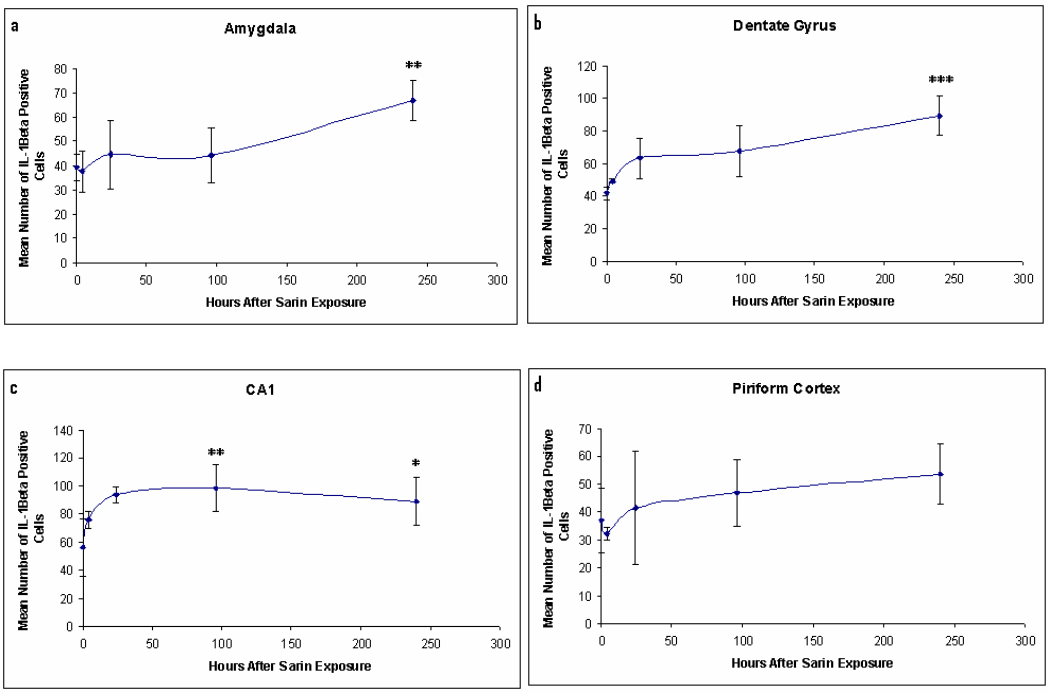

FIGURE 15. Temporal Changes in IL-1β Expression After 24µg/kg Sarin in Four Brain Regions: The plotted values represent the mean number of IL-1β-positive cells ± S.D. in the (a) amygdala, (b) dentate gyrus, (c) CA1 hippocampus, and (d) piriform cortex of mice given 24µg/kg sarin at four hours, 24 hours, four days and ten days post-dose. $F_{4,14}$= 6.625 for amygdala, $F_{4,14}$= 9.853 for dentate gyrus, $F_{4,14}$= 4.358 for CA1, and $F_{4,14}$= 1.754 for piriform cortex. A p-value <0.05 was considered significant (* $p<0.05$, ** $p<0.01$, *** $p<0.001$).

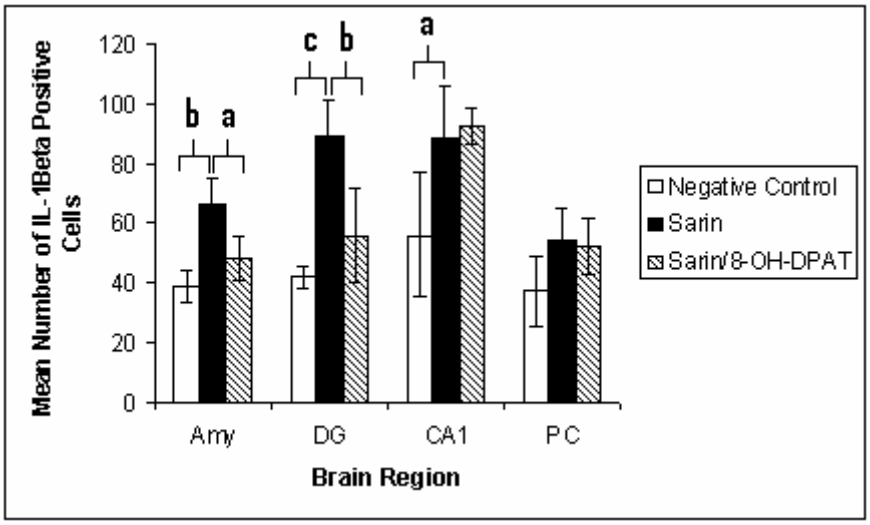

FIGURE 16. IL-1β Activity 10 Days after Treatment with Sarin and 8-OH-DPAT: Graph showing the mean number of IL-1β-positive cells in amygdala, dentate gyrus, CA1 hippocampus and piriform cortex ten days after treatment. Negative control mice were dosed with glycol and saline, sarin mice received 24μg/kg sarin, sarin/8-OH-DPAT mice received 24μg/kg sarin and 1.7mg/kg 8-OH-DPAT. Each bar represents the mean ± S.D. $F_{2,12}$= 17.27 for amygdala, $F_{2,12}$= 18.44 for dentate gyrus, $F_{2,12}$= 8.078 for CA1, and $F_{2,12}$= 3.380 for piriform cortex. A p-value <0.05 was considered significant (a = $p<0.05$, b = $p<0.01$, and c = $p<0.001$).

IV. DISCUSSION

The main objective of this study was to determine if sarin would have an adverse affect on specific brain regions. Specifically, we asked two questions; 1) does sarin cause inappropriate cell death; and 2) does an immune response occur as a result of sarin exposure? To answer these questions, we analyzed neurodegeneration and neuro-inflammation in sarin-treated mice using four specific techniques; 1) Fluoro-Jade C staining for degenerating neurons; 2) TUNEL staining for degraded DNA; 3) caspase-3 staining for cells undergoing apoptosis; and 4) IL-1β staining for cells undergoing an inflammatory response.

NEURODEGENERATION

Fluoro-Jade stain is a marker for neurons undergoing degeneration. Schmued and colleagues (2005) found that the newest generation of Fluoro-Jade (Fluoro-Jade C, FJ-C) shows lower background and higher staining intensity than its predecessors (FJ and FJ-B). Therefore, we used Fluoro-Jade C in our study. Using our C57Bl/6J mouse model of sarin exposure, FJ-C did not show the expected abundance of degenerating neurons. Some positively stained neurons were detected, particularly in the dentate gyrus at four days after sarin exposure, while there were a few scattered cells visible in amygdala, CA1 hippocampus and piriform cortex. The small number of FJ-C positive neurons visualized in the C57Bl/6J mouse model is consistent with the findings of McLin and Steward (2006), who used kainic acid (KA) to induce seizures and neurodegeneration in various

strains of mice and compared FJ-C staining across the different strains. They concluded that, not only were the C57Bl/6 mice particularly resistant to KA-induced seizures, but that this strain also showed little neurodegeneration (exemplified by very little FJ-C staining) when compared with other strains given similar KA treatments (McLin and Steward, 2006). Generally, KA-induced seizures produce similar excitotoxic neuronal damage to that caused by sarin-induced seizures. Seizure activity is required for the onset of neuronal damage in animal models of OP toxicity (Munro et al., 1994). Despite limiting their samples to only mice who underwent repeated tonic clonic seizures, McLin and Steward (2006) still detected very little FJ-C staining in the hippocampus of C57Bl/6 mice in comparison with other strains of mice whose neurodegeneration was far more pronounced (Figure 17). Based on the results of McLin and Steward and on our own results, we concluded that the C57Bl/6J mouse model may not be the optimal model for studying the effects of sarin on neurodegeneration, specifically that measured by FJ-C. In our study, neurodegeneration could not be quantified using FJ-C staining due to the relatively small number of positively-labeled cells. Despite the shortcomings of the animal model, the presence of a small number of dying neurons visualized with Fluoro-Jade C convinced us that further pursuit of this study was warranted.

TUNEL LABELING

During apoptosis and oncosis (Dong et al., 1997) the nuclear DNA of cells can be cleaved into multiples of ~180 base pairs. The TUNEL technique labels the ends of these cleaved nuclear DNA segments, allowing them to be identified by light microscopy.

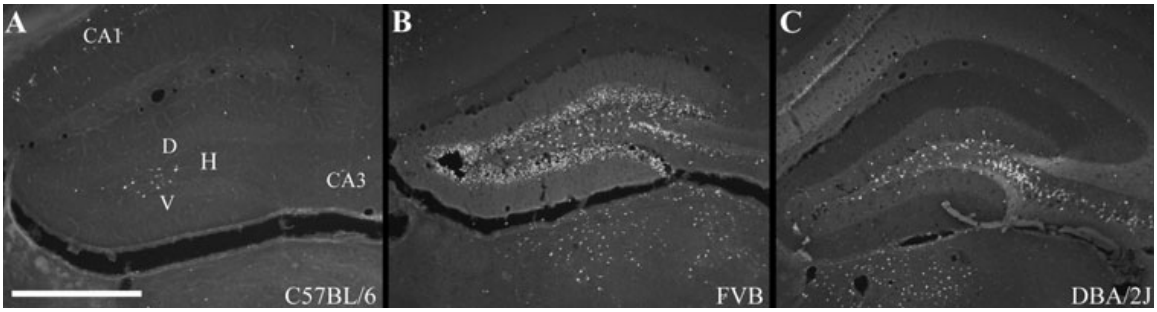

FIGURE 17. High power magnification (10X) photomicrographs of fluoro-jade stained tissue sections from mice of three strains: (A) C57BL/6, (B) FVB/N and (C) DBA/2J. Each section shows the dentate gyrus of the hippocampus of the right hemisphere. Portions of the CA1 and CA3 subfields are visible. The letters 'D' and 'V' denote the dorsal and ventral blades of the dentate gyrus and 'H' is the hilus region of the dentate gyrus. Degenerating cells are shown as bright punctuate points. Scale bar, 200μm (in A, applies to A-C). (Figure and associated legend are used with permission of the Editor, *European Journal of Neuroscience*.) (McLin and Steward, 2006)

Since TUNEL assay can detect both apoptotic and oncotic cell death (Trump et al., 1997), TUNEL labeling is currently used in conjunction with detection of another apoptosis-specific protein, i.e., caspase-3, to definitively determine apoptotic state. The relatively high background staining observed in all four brain regions is likely a result of the small sample sizes and could potentially be alleviated by increasing the number of negative control animals examined or by reporting the results as percentage of total cell counts rather than mean cell counts. The results of TUNEL staining of the brain tissue of mice indicated that the region most sensitive to sarin exposure was the dentate gyrus, where significant increases in staining occurred at four hours, four days and ten days after acute exposure. Consistent with the report that organophosphorus ester-induced seizures are initiated in the piriform cortex, there was a significant increase in staining in this region at the four hour time point, after which the staining decreased to non-significant levels (McDonough and Shih, 1997). This suggests that sarin had an effect on this region that was not long lasting, since more cells did not appear to be stained at later time points. After the initiation of seizures in the piriform cortex, other brain regions begin participating in the excitatory activity of the seizures as they are distally stimulated (McDonough and Shih, 1997). This is in agreement with our data that showed significant increases in neurodegeneration in the dentate gyrus and amygdala at later time points. Curiously, the dentate gyrus also showed an initial significant increase in TUNEL staining at four hours post-sarin dose, suggesting that this region is affected early after acute sarin exposure. A slight, non-significant increase in TUNEL labeling was observed in CA1 and piriform cortex regions, accompanied by a significant increase in the dentate gyrus at the ten day post-sarin dose time point, indicating that there may be an increasing

amount of cell death as time progresses. Gradually increasing cell death could be the result of an ongoing inflammatory response in the tissue. There may be an even greater increase in neurodegeneration at timepoints beyond ten days after exposure.

CASPASE-3 ACTIVITY

Apoptosis is a term that describes a complex sequence of events that ultimately lead to the death of a cell. During this process, specific enzymes that reside in every cell are activated and digest or cleave more enzymes, other proteins and DNA, finally resulting in one specific enzyme, i.e., capsase-3, becoming active. Activated caspase-3 is an effector molecule, responsible for carrying out the final death plans of the cell. Since nearly all apoptotic cell death utilizes caspase-3, it has become the signature molecule for the identification of apoptotic cells. We expected to see a unified activation of caspase-3 accompanied by TUNEL labeling early in the process of neurodegeneration. Both caspase activity and TUNEL labeling are expected to decrease as apoptotic cells die and are phagocytized. Due to the relatively small n, the unexpectedly high number of caspase-3-positive cells observed in our negative controls may be a statistical fluke. Background may be decreased to expected values with analysis of a larger n, or if positive staining is reported as percent of total cell count. Consistent with the observation that sarin-induced seizures are initiated within the piriform cortex, there was an early significant increase in caspase-3 activity at the 24 hour post-dose timepoint in that brain region (McDonough and Shih, 1997). This is subsequent to the significant increase in TUNEL labeling at the four hour post-dose timepoint in piriform cortex. This sequence is contrary to expectations based on the sequence of events during apoptosis,

where one would expect to observe simultaneous increases in effector caspase activity and TUNEL labeling. The four day post-dose time point showed a significant increase in caspase-3 staining in the dentate gyrus, implicating its role in sarin-induced excitotoxicity. In addition to the observed statistically significant caspase-3 staining, all four brain regions of interest showed slightly greater staining than negative controls with the exception of the four hour time points in the dentate gyrus and piriform cortex, indicating that apoptosis does play a role in neurodegeneration due to sarin exposure. It appears that caspase-3 activity gradually decreases after the peak seen at either four or 24 hours post-dose. This is in contrast to the gradual increase in TUNEL staining that we observed in our model (Figure 18). Apoptotic cells are expected to exhibit a simultaneous increase in effector caspase activity and DNA cleavage, rather than the staggered pattern observed in our data, indicating that apoptosis may play only a minor role in sarin toxicity.

IMMUNE RESPONSE

INTERLEUKIN-1β EXPRESSION

IL-1β is a proinflammatory cytokine whose expression in a cell is indicative of an ongoing inflammatory response. The toxic by-products of a prolonged neuro-inflammatory response can cause damage to nearby neurons. As much as a 2-fold change of IL-1β expression was observed in the brain tissue of sarin-exposed mice. Significant staining was observed first in the CA1 hippocampal region at four days after sarin treatment. At the ten day time point there was a significant increase in staining over negative control in the amygdala, dentate gyrus and CA1 regions. This came after a

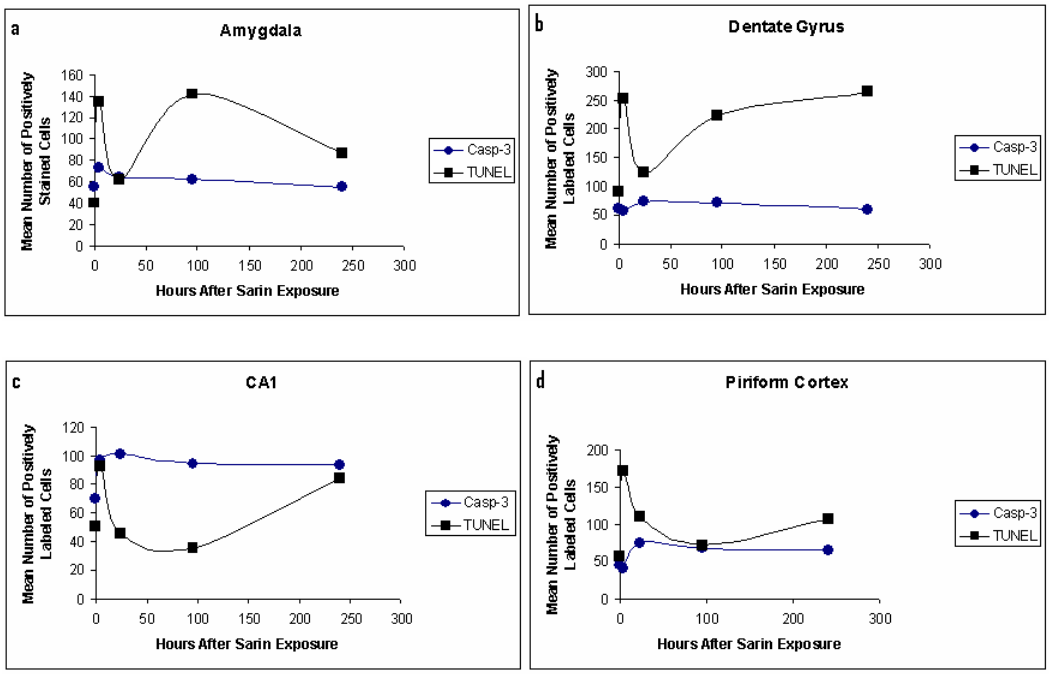

FIGURE 18. Comparison of TUNEL and Caspase-3 Labeling: The plotted values represent the mean number of Caspase-3 and TUNEL-positive cells in the (a) amygdala, (b) dentate gyrus, (c) CA1 hippocampus, and (d) piriform cortex of mice given 24µg/kg sarin at four hours, 24 hours, four days and ten days post-dose. Caspase-3 data points are represented by circles and TUNEL data points are represented by squares. Note the gradual decrease in caspase-3 activity observed at the later time points in all four brain regions. This is in contrast with the gradual increase in TUNEL labeling seen in all regions except the amygdala. The lack of agreement between these two staining techniques indicates that apoptosis is not the only type of cell death occurring in this animal model of sarin toxicity.

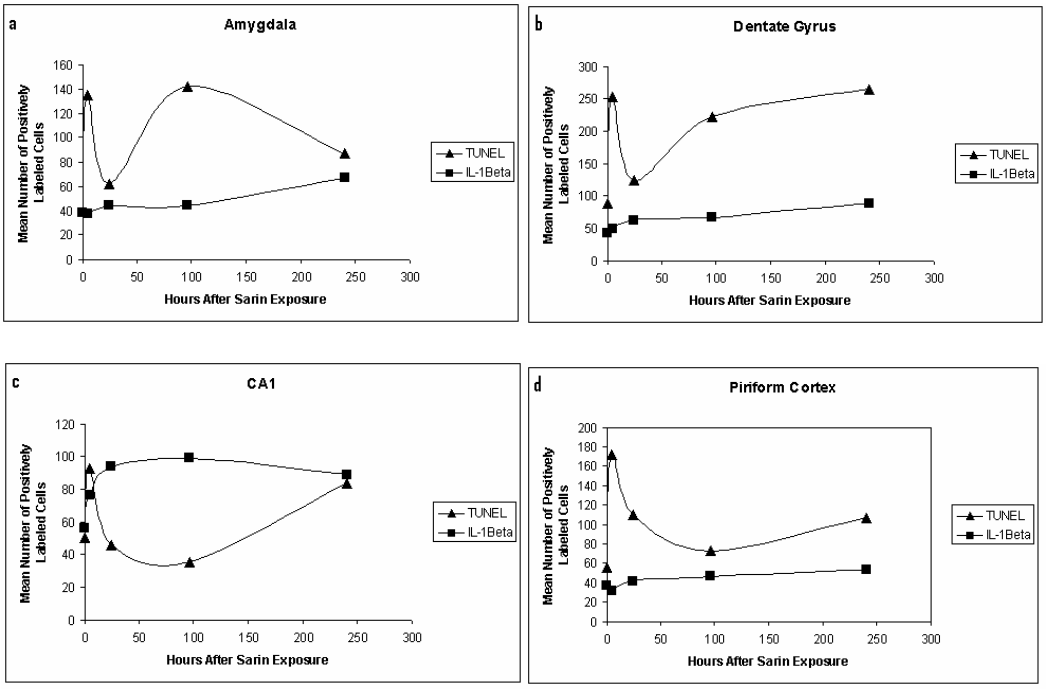

FIGURE 19. Comparison of TUNEL and IL-1β Labeling: The plotted values represent the mean number of IL-1β and TUNEL-positive cells in the (a) amygdala, (b) dentate gyrus, (c) CA1 hippocampus, and (d) piriform cortex of mice given 24μg/kg sarin at four hours, 24 hours, four days and ten days post-dose. TUNEL data points are represented by triangles and IL-1β data points are represented by squares. Note the gradual increase in TUNEL staining at the later time points in all regions except amygdala, and the corresponding gradual increase in IL-1β expression at later time points in all regions except CA1 hippocampus. This is indicative of the ongoing neurodegeneration and inflammatory response occurring in the tissue as late as ten days after a single exposure to sarin. (TUNEL data repeated from Figure 18.)

gradual increase in staining over time that was not statistically different at the earlier time points. Observation of this increasing IL-1β expression is indicative of the initiation of an inflammatory response in the tissues affected by sarin exposure. Of particular interest is the observation of a significant decrease in IL-1β expression (from the sarin treated mice) in the amygdala and dentate gyrus ten days after treatment with sarin and the 5-HT_{1A} receptor agonist 8-OH-DPAT. This is a direct indication that there is a decrease in inflammation after sarin exposure with 8-OH-DPAT treatment in these two regions of the brain. Based on the potential mechanisms of 5-HT_{1A} receptor agonist efficacy, and the known progression of sarin-induced seizure activity, the most likely explanation for 8-OH-DPAT's anti-inflammatory effect is its decrease of glutamate release (Srkalovic et al., 1994). Since glutamatergic stimulation of NMDA receptors is a primary culprit in ongoing seizure activity (McDonough and Shih, 1997), prevention of glutamate release decreases or ends seizure activity, thereby attenuating the resultant neuroinflammation.

Also of interest is the gradual increase in IL-1β expression over time in the amygdala, dentate gyrus and piriform cortex (Figure 19). This correlates with the observed increase in TUNEL labeling and contrasts with the decrease in caspase-3 activity. This could be indicative of an increase in oncotic cell death, while apoptotic cell death is decreasing over time. The increasing presence of IL-1β corresponds with the fact that oncotic cell death causes an inflammatory reaction in local tissue. An alternative explanation is that the cells expressing IL-1β have been damaged by the acute sarin exposure, but are in the process of recovering from the insult, and the inflammatory response is a protective repair mechanism.

CONCLUSIONS

Exposure to a single s.c. injection of sarin causes neurotoxicity in C57Bl/6J mice given a dose of 1.5 mg/kg CBDP, a carboxylesterase scavenger. Neuronal excitotoxicity occurs as a result of sarin's irreversible binding of acetylcholinesterase (McDonough and Shih, 1997). The resultant cholinergic activity initiates seizures which are further carried on by glutamatergic stimulation of NMDA receptors (McDonough and Shih, 1997). This excitatory activity results in neuroinflammation and neuronal death (Chapman et al., 2006; Svensson et al., 2001; Abdel-Rahman et al., 2002). Apoptosis and oncosis likely both contribute to neuronal loss in our model of sarin toxicity. The dentate gyrus exhibited the greatest sensitivity to sarin, indicated by increased cell death. The amygdala and piriform cortex regions exhibit similar sensitivity to sarin, lower than that of the dentate gyrus, as indicated by TUNEL staining, whereas the CA1 hippocampal region is not significantly affected by sarin exposure. The temporal sequence of TUNEL and caspase-3 staining indicates that apoptotic cell death is certainly occurring as a result of sarin exposure but may not be the only mode of cell death employed under such circumstances. Caspase-3 expression, which definitively indicates apoptotic cell death, was significantly up-regulated in the piriform cortex 24 hours after acute sarin exposure. In contrast with our TUNEL results, the CA1 hippocampal region displayed significant caspase-3 activity four days after sarin injection. Dentate gyrus and amygdala did not show any significant caspase-3 activity. It would be beneficial to increase the number of timepoints examined early after sarin injection in order to determine the interplay and precise temporal arrangement of caspase-3 activity and TUNEL labeling in addition to

identifying the ideal time at which cell death could be targeted for therapeutic intervention.

Although the caspase-3 activity detected in our samples underwent an initial increase followed by a gradual decrease, IL-1β staining was indicative of a gradual increase in inflammatory activity following sarin exposure. Amygdala, dentate gyrus and CA1 hippocampal regions are susceptible to neuroinflammation as a result of sarin exposure, indicated by significant increases in IL-1β expression. The potential therapeutic value of 8-OH-DPAT was demonstrated by the significant decreases in IL-1β expression observed in the amygdala and dentate gyrus regions at ten days after sarin and 8-OH-DPAT injection. We suspect that the efficacy of 8-OH-DPAT treatment lies in its ability to attenuate glutamate release, thereby putting an end to seizure activity due to NMDA receptor stimulation.

Our TUNEL data indicate that there is a gradual increase in cell death over time after an acute exposure to sarin in the dentate gyrus, CA1 and piriform cortex regions. Although none of these values reached statistical significance, it is possible that they may at later time points. A similar increase in inflammation was observed in all regions except CA1 hippocampus. This correlation indicates that cell death, accompanied by an inflammatory response may be a persistent threat to neuronal function beyond ten days after an acute exposure to sarin. This observation is corroborated by Chapman and colleagues (2006), who reported that significantly up-regulated inflammatory cytokines were still detectable up to 30 days beyond a single exposure to sarin. Effector caspase activity, on the other hand, after an early peak at four or 24 hours post-exposure, gradually decreases over time, while TUNEL labeling of dying cells gradually increases.

This could be indicative of a shift from primarily apoptotic cell death to oncotic cell death as time progresses.

Further research should be done to obtain conclusive results on the temporal progression of cell death and inflammation in this model of sarin exposure. The time course should be extended in order to determine when neurodegeneration and neuroinflammation peak and the therapeutic value of 8-OH-DPAT should be examined at corresponding time points. Unfortunately, the ten day post-treatment time point was not optimal in all cases, and therefore the apparent ineffectiveness of 8-OH-DPAT treatment may be misleading. If all time points had been examined with 8-OH-DPAT treatment, more significant results may have been observed. It would also be beneficial to include more early time points to determine if there is a peak time during which apoptosis occurs in response to sarin exposure, possibly providing an additional therapeutic window. This work would create a broader view of the toxicity associated with sarin exposure and have applications in defense against terrorism and chemical warfare. These preliminary results indicate that 8-OH-DPAT may be an effective therapy against the neuroinflammation that occurs as a result of exposure to nerve agents. More work must be done at appropriately chosen timepoints in order to determine the efficacy of 8-OH-DPAT treatment against neuronal cell death.

V. APPENDIX

[redacted]	Animal Number	No. of Sections Counted			
		Amygdala	Dentate Gyrus	CA1	Piriform Cortex
Positive Controls	155	1	1	1	1
	156	1	1	1	1
	193	1	1	1	1
Negative Controls	155	2	2	2	2
	156	2	2	2	2
	178	1	1	1	1
	193	2	2	2	2
CBDP Only 4 Hours Post-Treatment	130	1	1	1	1
	131	1	1	1	1
	132	1	1	1	1
	133	1	1	1	1
Sarin + CBDP 4 Hours Post-Treatment	158	2	2	2	2
	159	1	1	1	1
Sarin + CBDP 24 Hours Post-Treatment	210	2	2	2	2
	212	2	2	2	2
Sarin + CBDP 96 Hours Post-Treatment	146	1	1	1	1
	147	1	1	1	1
	148	1	1	1	1
	149	1	1	1	1
Sarin + CBDP 240 Hours Post-Treatment	175	0	2	2	2
	177	1	1	1	1
	185	1	1	1	1
	189	1	1	1	1
	192	0	1	1	1
Sarin + CBDP + 8-OH-DPAT 240 Hours Post-Treatment	219	1	1	1	1
	220	1	1	1	1
	221	1	1	1	1
	222	1	1	1	1
	224	1	1	1	1
	225	1	1	1	1

TABLE 1. Number of Sections Assessed for TUNEL Labeling: This table summarizes the number of sections that were TUNEL-labeled and counted for each animal within the

experimental groups. Positive controls were stained to confirm that the assay protocol was performed properly, however counts were not included in the statistical analysis. Counts from multiple sections from each animal were averaged to obtain a mean cell count for each region. Regions with 0 sections counted (gray boxes) were disregarded as a result of damage to the section making an accurate cell count impossible.

[redacted]	Animal Number	No. of Sections Counted			
		Amygdala	Dentate Gyrus	CA1	Piriform Cortex
Negative Controls	180	2	2	2	2
	181	2	2	2	2
	184	2	2	2	2
	193	2	2	2	2
CBDP Only 4 Hours Post-Treatment	130	2	2	2	2
	131	2	2	2	2
	132	2	2	2	2
	133	2	2	2	2
Sarin + CBDP 4 Hours Post-Treatment	158	2	2	2	2
	159	2	2	2	1
Sarin + CBDP 24 Hours Post-Treatment	210	2	2	2	2
	212	2	2	2	2
Sarin + CBDP 96 Hours Post-Treatment	146	2	2	2	2
	153	2	2	2	2
	154	2	2	2	2
	161	2	2	2	2
Sarin + CBDP 240 Hours Post-Treatment	174	1	1	1	1
	177	2	2	2	2
	185	2	2	2	2
	189	2	2	2	2
	192	0	2	2	2
Sarin + CBDP + 8-OH-DPAT 240 Hours Post-Treatment	219	2	2	2	2
	220	2	2	2	2
	221	0	2	2	2
	222	2	2	2	2
	224	2	1	2	2
	225	2	2	1	2

TABLE 2. Number of Sections assessed for Caspase-3 Labeling: This table summarizes the number of sections that were caspase-stained and counted for each animal within the experimental groups. Counts from multiple sections from each animal were averaged to obtain a mean cell count for each region. Regions with 0 sections counted (gray boxes) were disregarded as a result of damage to the section making an accurate cell count impossible.

[redacted]	Animal Number	No. of Sections Counted			
		Amygdala	Dentate Gyrus	CA1	Piriform Cortex
Negative Controls	180	2	2	2	2
	181	2	1	2	2
	184	2	1	1	2
	193	2	2	2	2
CBDP Only 4 Hours Post-Treatment	130	1	2	2	2
	131	2	2	2	2
	132	2	2	2	2
	133	2	2	2	2
Sarin + CBDP 4 Hours Post-Treatment	158	2	2	2	2
	159	2	2	2	2
Sarin + CBDP 24 Hours Post-Treatment	210	2	2	2	2
	212	2	2	2	2
Sarin + CBDP 96 Hours Post-Treatment	144	2	2	2	2
	145	1	2	2	2
	146	2	2	2	2
	147	1	2	2	2
	148	2	2	2	1
	149	2	2	2	2
Sarin + CBDP 240 Hours Post-Treatment	175	2	1	1	2
	177	1	2	2	2
	185	2	2	2	1
	189	2	2	2	2
	192	2	2	2	2
Sarin + CBDP + 8-OH-DPAT 240 Hours Post-Treatment	219	1	2	2	2
	220	2	2	2	2
	221	1	1	1	1
	222	1	1	1	2
	224	2	2	2	2
	225	2	2	2	2

TABLE 3. Number of Sections Assessed for IL-1β Labeling: This table summarizes the number of sections that were stained for IL-1β and counted for each animal within the experimental groups. Counts from multiple sections from each animal were averaged to obtain a mean cell count for each region.

VI. REFERENCES

1. Abdel-Rahman, A., A.K. Shetty, and M.B. Abou-Donia, Acute exposure to sarin increases blood brain barrier permeability and induces neuropathological changes in the rat brain: dose-response relationships. Neuroscience, 2002. 113(3): p. 721-41.
2. Adayev, T., et al., Agonist stimulation of the serotonin1A receptor causes suppression of anoxia-induced apoptosis via mitogen-activated protein kinase in neuronal HN2-5 cells. J Neurochem, 1999. 72(4): p. 1489-96.
3. Basu, A., J.K. Krady, and S.W. Levison, Interleukin-1: a master regulator of neuroinflammation. J Neurosci Res, 2004. 78(2): p. 151-6.
4. Basu, A., et al., Interleukin-1 and the interleukin-1 type 1 receptor are essential for the progressive neurodegeneration that ensues subsequent to a mild hypoxic/ischemic injury. J Cereb Blood Flow Metab, 2005. 25:p.17-29.
5. Carlson, K. and M. Ehrich, Organophosphorus compound-induced delayed neurotoxicity in white leghorn hens assessed by Fluoro-Jade. Int J Toxicol, 2004. 23(4): p. 259-66.
6. Chalmers, D.T. and S.J. Watson, Comparative anatomical distribution of 5-HT1A receptor mRNA and 5-HT1A binding in rat brain--a combined in situ hybridisation/in vitro receptor autoradiographic study. Brain Res, 1991. 561(1): p. 51-60.

7. Chapman, S., T. Kadar, and E. Gilat, Seizure duration following sarin exposure affects neuro-inflammatory markers in the rat brain. Neurotoxicology, 2006. 27(2): p. 277-83.

8. Colino, A. and J.V. Halliwell, Differential modulation of three separate K-conductances in hippocampal CA1 neurons by serotonin. Nature, 1987. 328(6125): p. 73-7.

9. Damodaran, T.V., et al., Toxicogenomic studies of the rat brain at an early time point following acute sarin exposure. Neurochem Res, 2006. 31(3): p. 367-81.

10. Davies, C.A., et al., The progression and topographic distribution of interleukin-1beta expression after permanent middle cerebral artery occlusion in the rat. J Cereb Blood Flow Metab, 1999. 19(1): p. 87-98.

11. Dong, Z., et al., Internucleosomal DNA cleavage triggered by plasma membrane damage during necrotic cell death. Involvement of serine but not cysteine proteases. Am J Pathol, 1997. 151(5): p. 1205-13.

12. Fargin, A., et al., Effector coupling mechanisms of the cloned 5-HT1A receptor. J Biol Chem, 1989. 264(25): p. 14848-52.

13. Fietta, P., Many ways to die: passive and active cell death styles. Riv Biol, 2006. 99(1): p. 69-83.

14. Gupta, R.C., G.T. Patterson, and W.D. Dettbarn, Acute tabun toxicity; biochemical and histochemical consequences in brain and skeletal muscles of rat. Toxicology, 1987. 46(3): p. 329-41.

15. Henderson, R.F., et al., Response of rats to low levels of sarin. Toxicol Appl Pharmacol, 2002. 184(2): p. 67-76.

16. Hoskins, B., et al., Relationship between the neurotoxicities of Soman, Sarin and Tabun, and acetylcholinesterase inhibition. Toxicol Lett, 1986. 30(2): p. 121-9.

17. Kline, A.E., et al., The selective 5-HT(1A) receptor agonist repinotan HCl attenuates histopathology and spatial learning deficits following traumatic brain injury in rats. Neuroscience, 2001. 106(3): p. 547-55.

18. Liu, Y.F. and P.R. Albert, Cell-specific signaling of the 5-HT1A receptor. Modulation by protein kinases C and A. J Biol Chem, 1991. 266(35): p. 23689-97.

19. Majno, G. and I. Joris, Apoptosis, oncosis, and necrosis. An overview of cell death. Am J Pathol, 1995. 146(1): p. 3-15.

20. Maxwell, D.M., K.M. Brecht, and B.L. O'Neill, The effect of carboxylesterase inhibition on interspecies differences in soman toxicity. Toxicol Lett, 1987. 39(1): p. 35-42.

21. McDonough, J.H., Jr. and T.M. Shih, Neuropharmacological mechanisms of nerve agent- induced seizure and neuropathology. Neurosci Biobehav Rev, 1997. 21(5): p. 559-79.

22. McGeer, P.L. and E.G. McGeer, The inflammatory response system of brain: implications for therapy of Alzheimer and other neurodegenerative diseases. Brain Res Brain Res Rev, 1995. 21(2): p. 195-218.

23. McLean, M.J., et al., Prophylactic and therapeutic efficacy of memantine against seizures produced by soman in the rat. Toxicol Appl Pharmacol, 1992. 112(1): p. 95-103.

24. McLin, J.P. and O. Steward, Comparison of seizure phenotype and neurodegeneration induced by systemic kainic acid in inbred, outbred, and hybrid mouse strains. Eur J Neurosci, 2006. 24(8): p. 2191-202.

25. Medical management guidelines for nerve agents tabun (GA); sarin (GB); soman (GD); and VX., in Centers for Disease Control and Prevention. 2003, Agency for Toxic Substances and Disease Registry.

26. Munro, N., Toxicity of the Organophosphate Chemical Warfare Agents GA, GB, and VX: Implications for Public Protection. Environ Health Perspect, 1994. 102(1): p. 18-37.

27. Nyakas, C., et al., Selective decline of 5-HT1A receptor binding sites in rat cortex, hippocampus and cholinergic basal forebrain nuclei during aging. J Chem Neuroanat, 1997. 13(1): p. 53-61.

28. Ohman, J., R. Braakman, and V. Legout, Repinotan (BAY x 3702): a 5HT1A agonist in traumatically brain injured patients. J Neurotrauma, 2001. 18(12): p. 1313-21.

29. Okumura, T., et al., The Tokyo subway sarin attack: disaster management, Part 1: Community emergency response. Acad Emerg Med, 1998. 5(6): p. 613-7.

30. Oosterink, B.J., T. Harkany, and P.G. Luiten, Post-lesion administration of 5-HT1A receptor agonist 8-OH-DPAT protects cholinergic nucleus basalis neurons against NMDA excitotoxicity. Neuroreport, 2003. 14(1): p. 57-60.

31. Prehn, J.H., et al., Effects of serotonergic drugs in experimental brain ischemia: evidence for a protective role of serotonin in cerebral ischemia. Brain Res, 1993. 630(1-2): p. 10-20.

32. Ramos, A.J., et al., The 5HT1A receptor agonist, 8-OH-DPAT, protects neurons and reduces astroglial reaction after ischemic damage caused by cortical devascularization. Brain Res, 2004. 1030(2): p. 201-20.

33. Schmued, L.C., et al., Fluoro-Jade C results in ultra high resolution and contrast labeling of degenerating neurons. Brain Res, 2005. 1035(1): p. 24-31.

34. Smith, M.I. and M. Deshmukh, Endoplasmic reticulum stress-induced apoptosis requires bax for commitment and Apaf-1 for execution in primary neurons. Cell Death Differ, 2007. 14(5): p. 1011-9.

35. Srkalovic, G., et al., Serotonergic inhibition of extracellular glutamate in the suprachiasmatic nuclear region assessed using in vivo brain microdialysis. Brain Res, 1994. 656(2): p. 302-8.

36. Steward, O., et al., Neuronal activity up-regulates astroglial gene expression. Proc Natl Acad Sci U S A, 1991. 88(15): p. 6819-23.

37. Svensson, I., et al., Soman-induced interleukin-1 beta mRNA and protein in rat brain. Neurotoxicology, 2001. 22(3): p. 355-62.

38. Tanaka, K., S.H. Graham, and R.P. Simon, The role of excitatory neurotransmitters in seizure-induced neuronal injury in rats. Brain Res, 1996. 737(1-2): p. 59-63.

39. Tokuda, Y., et al., Prehospital management of sarin nerve gas terrorism in urban settings: 10 years of progress after the Tokyo subway sarin attack. Resuscitation, 2006. 68(2): p. 193-202.

40. Trump, B.F., et al., The pathways of cell death: oncosis, apoptosis, and necrosis. Toxicol Pathol, 1997. 25(1): p. 82-8.

41. Tu, B. and N.G. Bazan, Hippocampal kindling epileptogenesis upregulates neuronal cyclooxygenase-2 expression in neocortex. Exp Neurol, 2003. 179(2): p. 167-75.

42. Williams, A.J., et al., Central neuro-inflammatory gene response following soman exposure in the rat. Neurosci Lett, 2003. 349(3): p. 147-50.

43. Wood, P.L., Microglia: Roles of microglia in chronic neurodegenerative diseases, in Neuroinflammation: Mechanisms and Management, P.L. Wood, Editor. 2003, Humana Press: Totowa, NJ. p. 3-27.

44. Wyllie, A.H., Apoptosis: an overview. Br Med Bull, 1997. 53(3): p. 451-65.

45. Wyllie, A.H., G.J. Beattie, and A.D. Hargreaves, Chromatin changes in apoptosis. Histochem J, 1981. 13(4): p. 681-92.

46. Zimmer, L.A., M. Ennis, and M.T. Shipley, Soman-induced seizures rapidly activate astrocytes and microglia in discrete brain regions. J Comp Neurol, 1997. 378(4): p. 482-92.